



# **Surface Modification of Thin-Film-Composite Membranes with Antibiotics for Fouling Reduction**

**Maryam Golestani**

Submitted in fulfilment of requirement for  
The Master of Research  
(9-month research program)

Department of Environmental Sciences  
Macquarie University, Sydney, Australia

October 2018

## ***Declaration***

This thesis is a presentation of my original research work. Wherever contributions of others are involved every effort is made to indicate this clearly, with due reference to the literature, and acknowledgment of collaborative research and discussion. This work has been done under the guidance of Dr. Shuaifei Zhao at the Macquarie University, Sydney, Australia.

Maryam Golestani

A handwritten signature in black ink, appearing to read 'Maryam' with a stylized flourish at the end.

## *Acknowledgements*

I express my sincere gratitude and profound regard to my supervisor Dr. Shuaifei Zhao for his guidance, encouragement, support and invaluable advice at every stage of this study.

I wish to express my special thanks to Prof. Damian Gore, Prof. Vladimir Strezov and Dr. Tao Kan for allowing me to use the laboratory facilities and assisting me in the lab works.

I would like to acknowledge Dr. Anahit Penesyan and Mark Tran from department of molecular sciences for their kind assistance to use their lab instrument and facilities.

## **List of tables**

Table 1. Concentration and deposition time of TOB and PDA in different modified membranes

Table 2. Water contact angles of the virgin and modified TFC membranes

Table 3. Water fluxes and salt rejections of the virgin and modified membranes

Table 4. Absorbance of the cultivated bacteria solution for different membrane samples

## List of Figures

Fig. 1. Relative capacity of installed desalination technologies

Fig. 2. Schematic illustration of a TFC polyamide membrane

Fig. 3. a) Hydration layer on a hydrophilic surface and the prevention of foulants attachment, b) Gibbs free energy changes before, when and after the adsorption of foulants on ordinary and hydrophilic membrane surfaces

Fig. 4. Effect of biocide incorporation into the membrane surface, improving the antifouling properties

Fig. 5. Mechanism of self-assembly of TiO<sub>2</sub> nanoparticles to the functional groups of PA

Fig. 6. Attachment of TOB molecules to an RO membrane functional group

Fig. 7. a) Schematic illustration of a possible mechanism of dopamine polymerization. b) Deposition process of PDA on the substrate surface

Fig. 8. PDA functionality in membrane modification

Fig. 9. Schematic illustration of the synthesis of polyethylene glycol conjugated tobramycin

Fig. 10. Schematic of TFC membrane surface modification via coating with TOB in PDA matrix

Fig. 11. Schematic of the dead-end cell filtration setup

Fig. 12. The color of TOB/dopamine (a,b,c) and dopamine (d,e,f) solution in tris buffer solution (pH:8.5) on top of the membrane surface during coating process after 5min, 45 min, and 90min from left to right

Fig. 13. UV-vis spectra of (a) dopamine (2 g/l) in Tris (pH: 8.5), (b) TOB (2 g/l) + dopamine (2 g/l) in Tris (pH: 8.5), and (c) Time dependent absorbance of dopamine solutions at 400 nm

Fig. 14. FESEM images of the virgin and modified membranes (M1, M\*2, M3, and M4)

Fig. 15. Roughness parameters for the virgin and modified membranes. R<sub>q</sub> represents the root mean square and R<sub>a</sub> is the average roughness.

Fig. 16. FT-IR spectra of the virgin and modified membranes in the range of a) 400-3400 cm<sup>-1</sup>, b) 1400-1600 cm<sup>-1</sup>

Fig. 17. Normalized flux change of the virgin and modified membranes with time during the filtration of BSA

Fig. 18. Visual images of the inhibition zone against *E.coli* bacteria indicated by red dotted circle for virgin and modified membranes (left) M3 modified membrane (right)

Fig. 19. CLSM images of *E.coli* on the virgin and modified membranes after 4-h (left) and 24-h (right) cultivation, the black background is the membrane surface and green points are stained bacteria

## Table of content

|   |    |
|---|----|
| 1. Introduction.....  | 2  |
| 2. Literature review .....                                      | 5  |
| 2.1. Thin film composite membranes .....                        | 5  |
| 2.2. Fouling of TFC membranes.....                              | 6  |
| 2.3. Post-modification strategies .....                         | 7  |
| 2.3.1. Enhancing surface hydrophilicity .....                   | 8  |
| 2.3.2. Changing electrostatic surface charge.....               | 10 |
| 2.3.3. Reducing surface roughness .....                         | 11 |
| 2.3.4. Using the steric repulsion effect.....                   | 12 |
| 2.3.5. Introducing antibacterial surface.....                   | 12 |
| 2.4. Biomimetic adhesive polydopamine .....                     | 15 |
| 3. Experimental .....   | 18 |
| 3.1. Materials.....   | 18 |
| 3.2. Surface modification of TFC membrane .....                 | 18 |
| 3.3. Membrane characterization .....                            | 20 |
| 3.3.1. Water contact angle .....                                | 20 |
| 3.3.2. Field emission scanning electron microscopy (FESEM)..... | 20 |
| 3.3.3. Fourier transform infrared (FTIR) spectroscopy .....     | 20 |
| 3.3.4. UV-visible spectroscopy .....                            | 21 |
| 3.3.5. Atomic force microscopy (AFM).....                       | 21 |
| 3.4. Water permeability and salt rejection of membranes .....   | 21 |
| 3.5. Organic fouling test .....                                 | 22 |
| 3.6. Antibacterial test.....                                    | 22 |
| 3.7. Anti-biofouling Properties .....                           | 23 |
| 4. Results and discussion .....                                 | 25 |

|  |    |
|--|----|
| 4.1. Membrane characterization .....                 | 25 |
| 4.1.1. Dopamine reactivity.....                      | 26 |
| 4.1.2. Morphology analysis.....                      | 28 |
| 4.1.3. Surface hydrophilicity.....                   | 30 |
| 4.1.4. Analysis of membrane chemical structure ..... | 31 |
| 4.2. Membrane permeability and salt rejection .....  | 33 |
| 4.3. Organic fouling evaluation .....                | 34 |
| 4.4. Anti-biofouling properties .....                | 35 |
| 5. Conclusion .....                                  | 41 |
| Reference .....                                      | 43 |

## Abstract

Thin-film-composite (TFC) membranes are used in reverse osmosis (RO) and nanofiltration (NF) for producing fresh water. However, they are prone to fouling by biological and chemical contaminants, which significantly diminishes their efficiency. Therefore, feed pretreatments and membrane cleaning are required to maintain their proper functionality, which increase operational cost. Alternatively, the surface properties of TFC membranes can be modified to reduce fouling and increase membrane efficiency and lifetime.

This project aimed to modify a commercial TFC membrane's surface with polydopamine (PDA) mixed with an antibiotic tobramycin (TOB). Polymerization reactivity of dopamine was identified by UV-vis spectroscopy. The modified-TFC membranes were characterized by scanning electron microscopy, atomic force microscopy, and water contact angle analysis. The separation performance, antifouling and antibacterial properties of the membranes were also examined.

The modified membranes showed antibacterial properties against *E.coli* and less flux reduction during filtration with bovine serum albumin (BSA) solution. The permeability and selectivity of the membrane after surface modification changed little. These results demonstrate that TOB can be directly deposited on TFC membranes using PDA as a matrix. Surface modification with TOB and PDA is an effective strategy to improve the organic fouling and biofouling resistance of TFC membranes.



## 1. Introduction

The world is witnessing fast industrialization, urbanization, population explosion, and climate change. It is becoming an increasing challenge to provide fresh and non-contaminated water for human communities as well as animals. However, there are promising separation technologies available in the market that can be used to produce fresh water from sea or brackish water. Multi-stage flash (MSF), multi-effect distillation (MED), and vapor compression (VC) are among the popular desalination processes to generate fresh water. Nevertheless, such technologies are highly uneconomical due to the high demand of energy for their operation (Li and Wang, 2010). In this regard, membrane technology, specifically for water desalination, is considered very promising to ameliorate this challenge to a greater extent (Buonomenna, 2013). Although, many Middle Eastern countries have been using the primary evaporation-based desalination technologies because of their access to the fuel resources, this has been overtaken globally by membrane technology in recent decades due to increasing energy costs (Asadollahi et al., 2017). Fig. 1 compares the total installed capacity of different technologies used for desalination (IDA Desalination Yearbook 2013–2014).

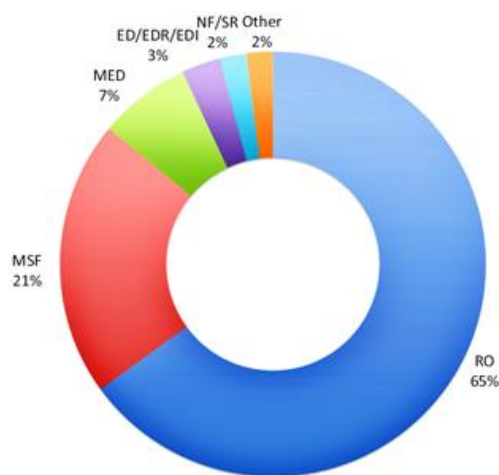


**Fig. 1.** Relative capacity of installed desalination technologies (IDA Desalination Yearbook 2013–2014).

Currently, the most common membranes used for desalination (e.g. reverse osmosis or nanofiltration membranes) are thin-film-composite (TFC) membranes due to the high salt rejection and water permeability, excellent thermal and chemical resistance, and mechanical strength. However, TFC membranes have two significant drawbacks. Namely, they are intolerant to oxidants (e.g. sodium hypochlorite) and susceptible to fouling.

Membrane fouling can be attributed to all particles, colloids, salts, and microorganisms deposited on a membrane surface. This phenomenon significantly decreases membrane performance by reducing water flux and degrading the polymeric membrane over time. Because of fouling, transmembrane pressure has to be increased, leading to higher energy consumption. Temporary fouling can be removed by washing allowing continuous use of a membrane, but permanent fouling results in membranes being unable to be restored (Zhao et al., Ong et al., 2016). As a result, modification of membranes is essential to improve the antifouling properties and to maintain high performance of the membranes.

Since the birth of TFC membranes, research has focused on developing a membrane with high performance or improving the surfaces of commercial membranes. Previous studies have proved that the physicochemical properties of TFC membrane surfaces, such as hydrophilicity, roughness, and electrostatic charges, are responsible for membrane fouling. Moreover, exerting steric effects using a long-chain polymer and the incorporation of biocides, such as nanoparticles can reduce membrane fouling properties (Li et al., 2017).

## **Research gaps and aims**

As shown in recent studies, one of the most common problems of TFC membranes in water treatment is biofouling (Karkhanechi et al., 2014a). Although disinfectants, such as chlorine, can reduce bio-fouling, they have adverse effects on TFC membranes due to damaging the polymeric membrane and reducing their performance. Alternatively, a reliable approach to reduce bio-fouling is by introducing an inherent antifouling property to the membrane surface. To address this problem, considerable research was devoted to applying nanoparticles to exert the antibacterial properties to the membrane surface. Biocidal nanoparticles such as Ag (Yin et al., 2013), TiO<sub>2</sub> (Zhang et al., 2017) and Cu (Ma et al., 2017) were applied on TFC membranes by different methods and their antifouling properties were investigated. However, there is still not sufficient research on synthesized antibiotics, which can react more effectively than nanoparticles. Moreover, nanoparticles are so small and likely to pass through membranes and enter the permeate water which may cause secondary contamination.

In this study, we aim to develop an antifouling and antibacterial TFC membrane by surface modification with a model antibiotic tobramycin (TOB). First, we modified the membrane surface to

obtain an anti-adhesive surface by increasing the hydrophilicity of the membrane surface using polydopamine (PDA). Second, we incorporated an antibiotic onto the membrane surface to decrease bacteria attachment and proliferation. By applying two different approaches we expect to achieve an enhanced antifouling property. It is hypothesized that by using a simple method, PDA can be used both as a hydrophilicity improver and a TOB immobilizer onto the membrane surface (Qiu et al., 2018). The modified membrane is anticipated to have antibacterial properties against *E.coli* bacteria.

## **2. Literature review**

### **2.1. Thin film composite membranes**

Membrane separation is based on the presence of a semi-permeable membrane. Various membranes have been used for water treatment applications classified to microfiltration, ultrafiltration, nanofiltration (NF) and reverse osmosis (RO). Microfiltration membranes with pore sizes around 1  $\mu\text{m}$  are used to separate large colloids and microorganisms, while ultrafiltration membranes have smaller pores which can remove proteins and macromolecules. Among different membrane types, RO and NF membranes are relatively dense (nonporous) and can remove salts from water and be used for desalination. Desalination is a process of removing salts from seawater or brackish water in order to make it suitable for human and industrial use. In membrane desalination, water passes through a dense membrane and dissolved ions are rejected. The first RO membrane was invented by Leob and Sourirajan (1963) who showed cellulose acetate (CA) membranes can reject almost 99% of salt. However, CA membranes had low permeability and a decade later, Cadotte and his colleagues (1980) introduced polyamide membranes called thin film composite (TFC) membrane. Currently, TFC membranes are used in both RO and NF to remove ions from salted water. However, NF membranes are designed to remove multivalent ions rather than monovalent ions (R Choudhury et al., 2017). Dissolved ions in water are surrounded by water molecules, known as hydration, which leads to higher hydrated diameters of multivalent ions than those of monovalent ions (J. Miller et al., 2016).

In a typical TFC membrane, polyamide (PA) is the selective layer synthesized by interfacial polymerization on a microporous substrate (Asadollahi et al., 2017). In interfacial polymerization, a dense, thin polyamide layer responsible for salt rejection, is formed on the top of the substrate layer. Both the PA and substrate layers are further reinforced by a third polyester support layer. A layer of polysulfone ultrafiltration membrane cast onto a polyester layer is used as the porous support (Fig. 2).

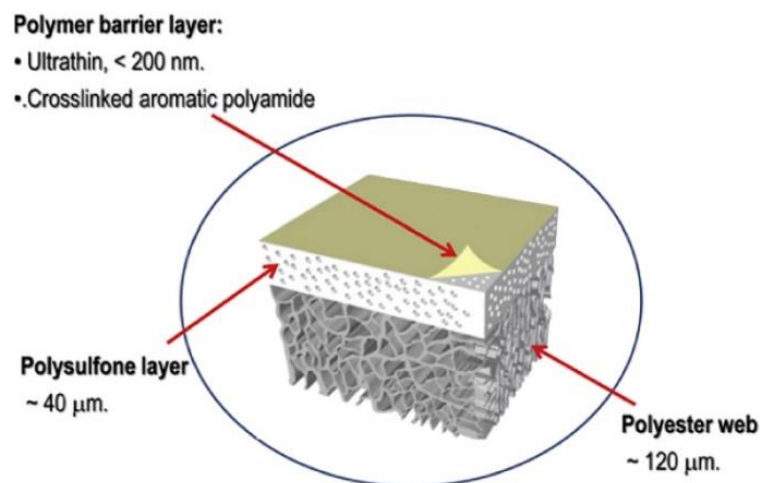


**Fig. 2.** Schematic illustration of a TFC polyamide membrane (Asadollahi et al., 2017)

## 2.2. Fouling of TFC membranes

While using a TFC membrane, due to transmembrane pressure, foulants can move to the membrane surface and attach to the membrane via electrostatic, hydrophobic, hydrogen-bonding or other interactions. In the next stage, foulants aggregate due to interactions between foulants and make a thick fouling layer on the membrane surface (Ong et al., 2016, Zhao et al., 2018). According to the foulant difference, fouling can be categorized into inorganic, organic and bio fouling.

Inorganic foulants consist of colloidal and dissolved substances. The most common colloids are silica, aluminum silicate and iron hydroxides and the less common colloids are aluminum oxide, manganese oxide and metal sulfides (Asadollahi et al., 2017). Dissolved inorganic salts, such as  $\text{CaSO}_4$ ,  $\text{CaCO}_3$ ,  $\text{SiO}_2$  and  $\text{BaSO}_4$ , may accumulate near the membrane surface due to rejection known as concentration polarization. When saturated salts exceed the saturation limit they start to crystallize and can result in scaling on the membrane surface. This increases the risk of fouling and decreases the permeation flux due to enhanced osmotic pressure (Shirazi et al., 2010). A reduction in scaling can be promoted by the addition of antiscalants, pH adjustment or increasing the crossflow velocity of the feed stream (Asadollahi et al., 2017).

Organic substances known as natural organic matters (NOM) are macromolecules that exist in surface or ground water. NOM are classified into colloidal ( $>0.45 \mu\text{m}$ ) and dissolved organic matters ( $<0.45 \mu\text{m}$ ) depending on their size (Asadollahi et al., 2017). Colloidal particles are one of the most problematic foulants since they cannot be easily removed by granular beds due to their small sizes

and electrostatic repulsion effect of the media. However, they can be mitigated using a coagulant-flocculating agent (Jiang et al., 2017). NOM comprises of a range of compounds from small hydrophobic acids, proteins and amino acids to larger humic and fulvic acids. The fouling mechanism is adsorption on the membrane surface and formation of a gel or cake layer (Asadollahi et al., 2017)

Among different types of membrane fouling, biofouling is an irreversible phenomenon which starts by the attachment of a few surviving planktonic bacteria followed by the growth and production of immature and mature biofilms (Nikkola et al., 2013). The reversible and irreversible adsorption steps are closely associated with organic fouling (He et al., 2016). A biofilm consists of attached microbial cells surrounded with a matrix of extracellular polymeric secretions (EPS) comprising proteins and glycoproteins for cells protection. Although biofouling can be significantly diminished by sodium hypochlorite washing, this is a problem for TFC polymeric membranes because of their sensitivity to chlorine degradation (Bjarnsholt et al., 2013, Misdan et al., 2016). As a result, studies have focused on applying substances such as biocides (Zhang et al., 2017), or polymers (Wang et al., 2015) on the membrane surface to reduce the attachment of bacteria.

Factors affecting membrane fouling can be summarised as (1) Operating conditions: pH, temperature, cross-flow velocity; (2) Solution properties: ionic strength and type, composition and concentration of foulants; and (3) Membrane properties: hydrophobicity, surface charge, and morphology (Abdelrasoul et al., 2013). Changing the properties of a TFC membrane can be applied either during the interfacial polymerization or after membrane preparation (i.e. post-modification). This thesis review will focus on post-modification strategies applied on prepared or commercial TFC membranes.

### **2.3. Post-modification strategies**

Membrane modification for fouling reduction refers to all efforts implemented for slowing down the attachment of foulants to the membrane surface and enhancing the flux recovery. It is believed that during the first stages of fouling, interactions between foulants and the surface govern the adsorption of foulant onto the membrane surface. As fouling progresses, the membrane surface becomes less accessible and foulant–foulant interactions become dominant (Meng et al., 2014). Surface modification of membranes can be achieved by one or a combination of different approaches

including (1) enhancing the membrane hydrophilicity, (2) reduction of surface roughness, (3) changing the membrane surface charge, (4) utilization of the steric repulsion effect, and (5) introduction of biocides. It should be noted that during modification, permeability and salt rejection should be maintained without any significant change.

These fouling mitigation approaches can be performed by incorporation of nano-particles, nanotubes, antibiotics and/or grafting and coating a zwitterionic, hydrophilic or antibacterial polymers via different methods.

Physically coated substances onto the membrane surface, including a noncovalent bond, can impart desirable characteristics by van der Waals or electrostatic interaction. This can be accomplished by layer-by-layer (LBL) (Ma et al., 2016) or dip coating (Louie et al., 2011) methods and more stable coating can be achieved by cross-linking (J. Miller et al., 2016). However, to obtain a long-term stability for the modification, surface-modifying agents should be covalently coupled to the PA surface. The PA layer of the TFC membrane contains unreacted carboxylic acid and amine groups on the surface which can be used for further grafting. Grafting refers to the addition of polymer chains onto the surface. If not enough functional groups exist on the membrane surface, additional reagents may be used to pretreat the surface for grafting. For example, a polymeric surface can be activated by ozone oxidation (Van Wagner et al., 2011b), redox initiators (Freger et al., 2002), plasma (H. Lin et al., 2010), or UV irradiation (Marré Tirado et al., 2016) to generate surface radicals. Recently, the use of polydopamine (PDA) as a bio-inspired adhesive has raised significant interest in TFC membrane surface modification. Due to the polar groups, such as hydroxyl and amine groups in PDA, it can promote the surface functionalization and immobilization (Zhang et al., 2013).

### **2.3.1. Enhancing surface hydrophilicity**

Chemistry of the membrane surface governs the membrane properties. Functional groups on the membrane surface make a surface hydrophilic or hydrophobic. In other words, a membrane can be attractive (hydrophilic) or repulsive (hydrophobic) to water when in contact with an aqueous solution. The hydrophilicity of a membrane can be determined by measuring the water contact angle between the membrane surface and a droplet of water. Hydrophilic membrane surfaces have a water contact angle  $\theta < 90^\circ$ . This property is attributed to the presence of active groups on the membrane surface that have the ability to form hydrogen-bonds with water molecules. As a result, a hydrophilic

membrane tends to absorb water molecules and make a layer of water in the vicinity of the contact surface, which will result in reduction of foulants attachment and interaction (Abdelrasoul et al., 2013). A large number of foulants, such as proteins and microorganisms, are naturally hydrophobic. Fig. 3a shows the hydration layer and the prevention of foulants attachment to a hydrophilic membrane surface. Although, TFC polyamide membranes are hydrophilic due to the unreacted hydroxyl group on the surface, more hydrophilic functional groups on the membrane surface show better antifouling properties (Zou et al., 2011).

Considering a thermodynamic system for membranes, water, and foulants, fouling behavior can be explained by Gibbs free energy (Zamani et al., 2016). Once foulants contact the membrane surface, Gibbs free energy is increased. According to the second law of thermodynamics, there is a natural tendency to achieve a minimum of the Gibbs free energy. The maximum Gibbs free energy with hydrophilic surfaces is higher than that with unmodified surfaces (He et al., 2016). As a result, foulants are less likely to attach to the surfaces of hydrophilic membranes (Fig. 3b).

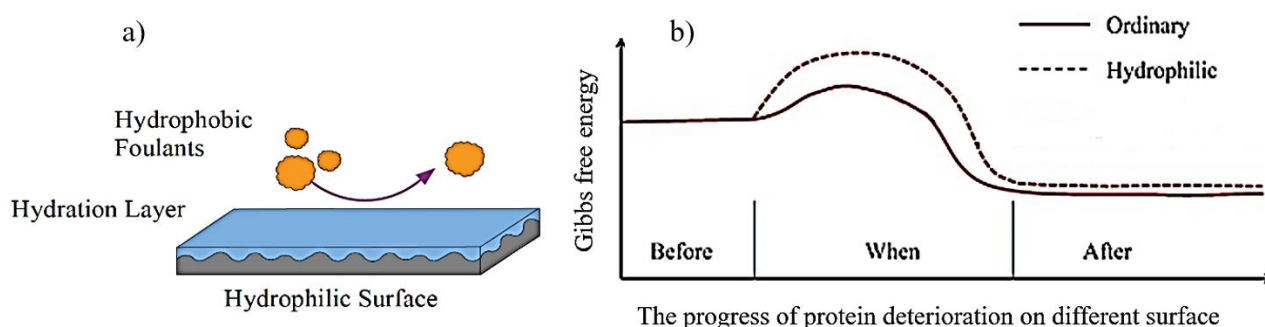


Fig. 3. a) hydration layer on a hydrophilic surface and the prevention of foulants attachment, b) Gibbs free energy changes before, when and after the adsorption of foulants on ordinary and hydrophilic membrane surfaces (He et al., 2016)

Applying a hydrophilic polymer on membrane surface, lessens the adsorption of protein and fouling formation (Zou et al., 2011). For instance, Sericin, a hydrophilic natural polymer with groups of hydroxyl, carboxyl and amino groups, was used to modify the surface of RO membrane by dip-coating followed by cross-linking with glutaraldehyde (GA) (Yu et al., 2013). The steady-state flux after 100 h filtration, showed 41.6% and 22.7% flux decline rates, for modified and unmodified membrane, respectively.

Polyethylene glycol (PEG), a neutral hydrophilic polymer, has been used as a coating layer for



preventing protein and bacterial adhesion to TFC membranes. Moreover, PEG derivatives grafted to RO membrane surface were more resistant to fouling in protein and cationic surfactant feeding solutions (Kang et al., 2011, Van Wagner et al., 2011a). The improved antifouling property is because of the increased hydrophilicity, neutral charge, and steric hindrance imparted by the long chain PEG molecules on the TFC membrane surface (Misdan et al., 2016). Similarly, polyvinyl alcohol (PVA) was covalently coated on a commercial TFC membrane (Hu et al., 2016). Water contact angle remarkably reduced from 60 of the virgin membrane to 40 of the modified membrane.

Zwitterionic coating can also significantly increases the membrane hydrophilicity (Chen et al., 2010). A zwitterionic membrane contains both positively and negatively charged functional groups, maintaining the neutral overall charge. This leads to stronger electrostatic interactions with water than hydrogen bonds of uncharged hydrophilic materials and higher energy is required to break these bounds (Karkhanechi et al., 2013, Chan et al., 2016, Azari and Zou, 2013). Azari et al. (2012), obtained a zwitterionic surface by depositing L-DOPA onto commercial membranes. Cross-flow filtration of BSA solution revealed less flux decline for the modified membranes compared to the virgin membrane.

A zwitterionic polymer, poly (styrene-co-4-vinylbenzophenone) (PSVBP), was grafted onto a commercial RO membrane by a  $K_2S_2O_8$ – $NaHSO_3$  redox system (Meng et al., 2014). Grafting PSVBP onto membrane surface improved membrane hydrophilicity and added negative charges onto the membrane surface. An excellent antifouling property against BSA during 50 h filtration was achieved. Water contact angle of the modified membrane significantly decreased after modification, indicating the excellent wettability of the PA-g-PSVBP membrane.

Similarly, a zwitterionic polymer was covalently immobilized on a TFC membrane by PDA (Karkhanechi et al., 2014b). The surface charge was changed from negative to neutral and the polymer noticeably increased the biofouling resistance of the TFC membrane due to the improved hydrophilicity.

### **2.3.2. Changing electrostatic surface charge**

The surface charge of membranes has important effects on fouling. Due to the electrostatic interactions, foulants are attracted onto the surface and fouling initiates when the foulants and surface

charge are not the same. Membranes become charged in contact with water due to the ionization of functional groups on the surface. Polyamide membranes have amphoteric properties due to the unreacted carboxylic acid and amine groups on the surface formed through interfacial polymerization. The zeta potential varies by operating pH, but under typical operating pH conditions ( $\text{pH} > 4$ ) the PA membrane has negative charges because of domination of its carboxylic groups. This can make a repulsive force to the negatively charged foulants and diminish their attachment to the surface. However, this effect can increase the attachment of positively charged foulants. In other words, the antifouling membrane should be developed according to the charge of foulants in the feeding water and cannot be used for all situation (Kang and Cao, 2012).

Furthermore, a membrane surface can become positively or negatively charged by coating or grafting a polymer with charged functional groups to the surface. For example, methacrylic acid (MA) as a representative of negatively charged groups was applied on a commercial TFC membrane. The modified membrane had a higher negative charge over the whole pH range because of the higher degree of dissociation of carboxylic groups. By increasing the grafting time, the flux decreased but salt rejection remained unchanged (Belfer et al., 1998, Belfer et al., 2001).

Polyethylene imine (PEI) was grafted onto the membrane surface to fabricate a positively charged RO membrane (Xu et al., 2015). The PEI-modified membrane showed high anti-fouling properties against the positively charged pollutants. Another positively charged RO membrane with improved salt rejection and water flux was prepared by depositing chitosan on a commercial RO membrane surface (Wei et al., 2010b).

Similarly, the fouling resistance of a coated RO membrane with hydrophilic PEG-based hydrogels against the charged surfactants was investigated by Sagle et al. (2009). The permeability of the modified membranes decreased while the salt rejection remained unchanged. Negatively charged membranes fouled extensively in the presence of positively charged surfactants and showed minimal fouling in the presence of negatively charged surfactants.

### **2.3.3. Reducing surface roughness**

Another important factor that affects the performance of RO membranes is the surface morphology, where smoother surfaces are less prone to fouling (Vrijenhoek et al., 2001). A

comparison between CA and TFC RO membranes indicated higher fouling rates for PA compared to CA membranes, due to higher surface roughness of PA membrane (Elimelech et al., 1997). Surfaces of polyamide membranes have inherent ridge-valley structures influenced by the manufacturing process, which increase accumulation of foulants on the surface. This property can be altered by applying additives during the polymerization process (Safarpour et al., 2015) or on the prepared membrane surface (post-modification) (Choi et al., 2013). Nanoparticles (NPs) help reduce membrane surface roughness by blocking the pores on the membrane surface. For example, it is reported that presence of graphene oxide (GO) in the polymerization solution during interfacial polymerization, leads to the reduction of membrane roughness and consequently better antifouling properties (Yin et al., 2016). Membrane surface roughness can also be influenced by the hydrophilicity and porosity of the support layer, which can be varied during the membrane polymerization process (Park et al., 2017).

#### **2.3.4. Using the steric repulsion effect**

Apart from the intrinsic properties, grafting a long-chain polymer to the membrane surface increased antifouling properties due to the steric repulsion mechanism formed by polymer brush. For instance, modified membranes grafted with Poly (ethylene glycol) diglycidyl ether (PEGDE) demonstrated improved fouling resistance to emulsions containing a charged surfactant, while the surface properties (e.g. surface charge, hydrophilicity and roughness) had little effects. This can be related to steric hindrance imparted by the PEG chains, preventing foulants from attaching to the membrane surface (Van Wagner et al., 2011b). When foulants come into contact with long-chain polymers, Gibbs free energy increases due to compressing the chains and lowering their motility. As a result, the thermodynamic system is likely to be recovered to a relaxed state and release foulants from the surface (He et al., 2016).

#### **2.3.5. Introducing antibacterial surface**

Another strategy for modifying membrane surfaces is applying biocidal effects. It is a safe method for killing bacteria near the surface and stop the bacteria proliferation. Applying biocides on the membrane surface leads to penetration of biocides into the bacteria' walls and killing them (Fig. 4). Antibacterial effects can occur either by passive or active strategies (Chudobova et al., 2013).

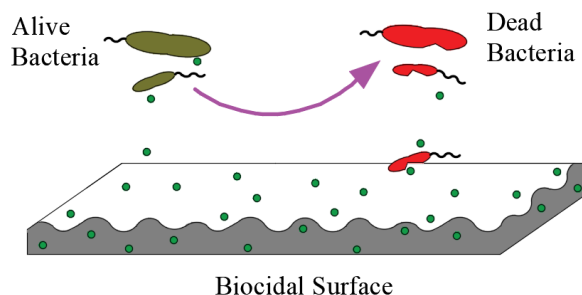
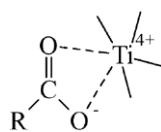


**Fig. 4.** Effect of biocide incorporation into the membrane surface, improving the antifouling properties

Titanium dioxide ( $\text{TiO}_2$ ) has been used to solve a number of water and air pollution problems due to its photocatalytic characteristics which are able to degrade organic pollutants and kill bacteria (Joost et al., 2015).  $\text{TiO}_2$  can be connected to PA membranes by forming a bidentate coordination between  $\text{Ti}^{4+}$  and two oxygen atoms of  $-\text{COOH}$  group or by H-bond between surface hydroxyl group of  $\text{TiO}_2$  and  $-\text{COOH}$  group of the membrane surface (Kim et al., 2003). Fig. 5 shows the mechanism of self-assembly of  $\text{TiO}_2$  nanoparticles on to the TFC membrane surface.

I. By a bidentate coordination of carboxylate to  $\text{Ti}^{4+}$ .



II. By a H-bond between carbonyl group and surface hydroxyl group of  $\text{TiO}_2$ .

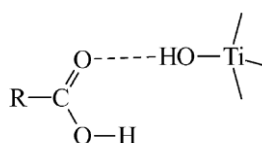


**Fig. 5.** Mechanism of self-assembly of  $\text{TiO}_2$  nanoparticles to the functional groups of PA (Kim et al., 2003)

Graphene oxide (GO) is a very effective hydrophilic material used as a potential efficient antioxidant in membrane modification which captures hydroxyl radicals to improve chlorine resistance (Choi et al., 2013). Due to nano-channels exist in GO layers, the permeability of membrane is increased (Ali et al., 2016). Previous studies showed that after surface modification by GO, membrane anti-fouling properties against protein, alginate or humic acid foulants were noticeably improved. (Han et al., 2016). Strong antimicrobial properties were also imposed to TFC polyamide membranes by the GO surface functionalization. GO was irreversibly bounded to the membrane using amide coupling between carboxyl groups of graphene oxide and carboxyl groups of the polyamide active layer. To convert the carboxyl groups ( $\text{R-COOH}$ ) to amine-reactive ester group ( $\text{R-CO-O-}$ ), the solution of *N*-(3-dimethylaminopropyl)-*N*'-ethylcarbodiimide (EDC) and *N*-hydroxysuccinimide (NHS) in MES buffer at pH 5 was put in contact with the membrane surface for 1 hour (Han et al.,

2016).

TiO<sub>2</sub> and graphene oxide (GO) nanoparticles were layer-by-layer self-assembled onto PA RO membrane surfaces by hydrogen bonding and physical absorption (Shao et al., 2017). Modified membranes demonstrated good anti-biofouling, chlorine resistance and improved hydrophilicity. Because of oxygen-containing groups, such as -COOH in GO, hydrogen bonds were formed with TiO<sub>2</sub>.

Ben-Sasson et al., introduced Ag-NPs (2014a) and Cu-NPs (2016), as antifouling agents, for modifying a TFC membrane surface by in-situ formation of nanoparticles from AgNO<sub>3</sub> and CuSO<sub>4</sub> with a reducing agent. With a minor impact on the membrane performance, the prominent antibacterial activity was demonstrated for modified membranes compared to the virgin membrane. There was an insignificant change in the surface charge and roughness after modification, but the surface became slightly less hydrophilic. In another study PEI was used as a capping agent for the synthesis of Cu nanoparticles. The positively charge Cu-NPs secreted from PEI amine groups were introduced to RO membrane surfaces via dip coating (Ben-Sasson et al., 2014b) or layer-by-layer coating, with assistance of negatively charged polyacrylic acid (PAA) (Ma et al., 2016).

Recently, an RO membrane surface was modified by applying hydrophilic tobramycin (TOB) and demonstrated a strong antimicrobial activity for the modified membrane (Wang et al., 2018). TOB is a potent antimicrobial agent used to treat various types of bacterial infections, particularly Gram-negative ones. RO membranes were prepared by interfacial polymerization and washed with 2,2,3,4,4,4-hexafluorobutyl methacrylate (PHFBM) in n-hexane (Wang et al., 2017). The amine group reacted with the remaining acyl chloride group on the membrane surface during the TOB grafting process. Fig. 6 shows how TOB reacts with functional groups on the surface of RO membranes.

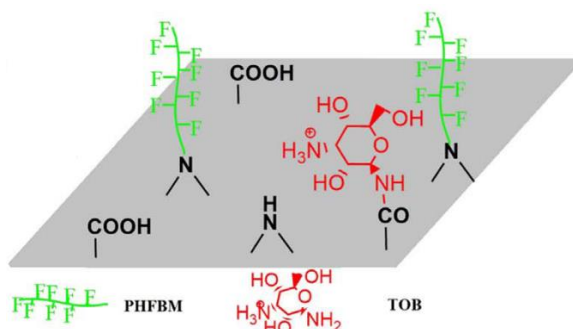


**Fig. 6.** Attachment of TOB molecules to an RO membrane functional group

## 2.4. Biomimetic adhesive polydopamine

Lee et al. (2007) introduced a material-independent and multifunctional surface coating using a catecholamine called dopamine hydrochloride (DA-HCl). They described the deposition of polydopamine (PDA) onto a variety of substrates including ceramics, metals and synthetic polymers, from an aqueous and buffer dopamine solution.

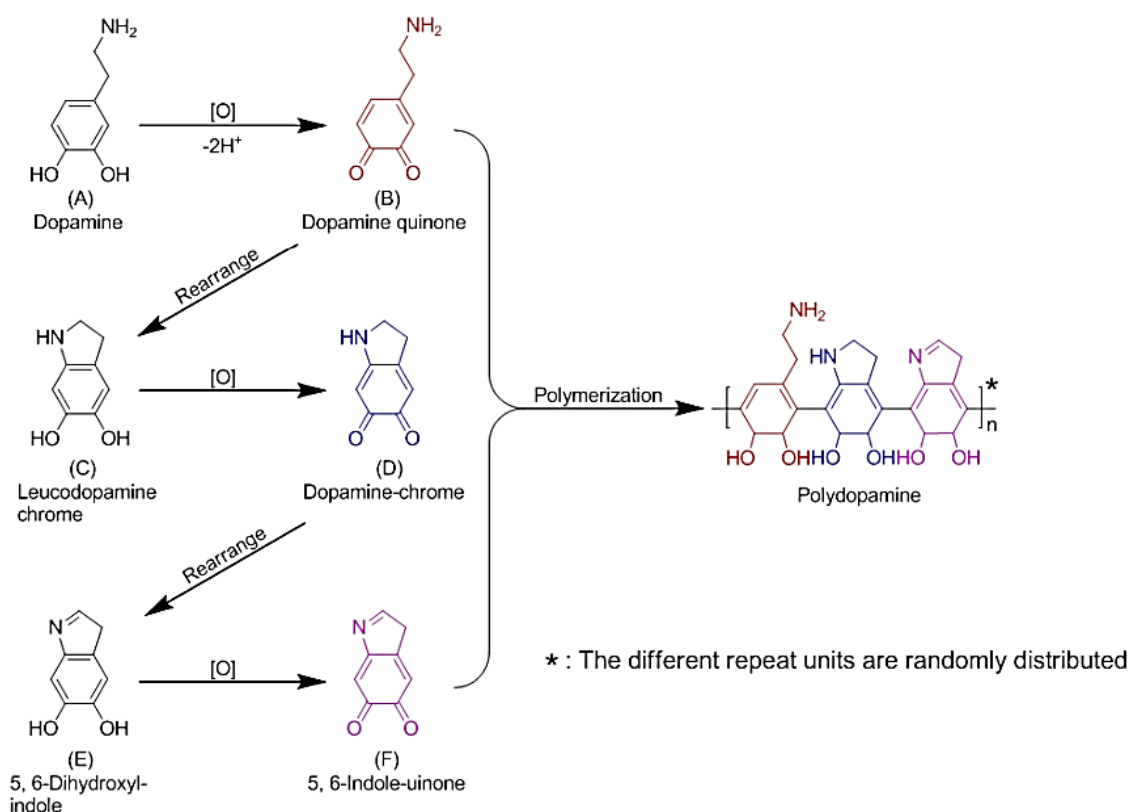
A dopamine molecule consists of a catechol structure (a benzene ring with two hydroxyl side groups) with one amine group attached via an ethyl chain. This small molecule is able to form a tight PDA layer in an aqueous solution, through self-polymerization in many environments, except in strongly alkaline conditions ( $\text{pH} > 13$ ) (Jiang et al., 2011). The polymerization mechanism of dopamine is not clearly known. Fig. 7 shows the possible structure of dopamine reaction in an aqueous solution. Dopamine is easily oxidized and after consecutive reactions, PDA particles are formed, and a highly adherent layer is generated on the substrate. Four to eight units of 5, 6-dihydroxyindole (E, in Fig. 7 a) make oligomers, which then are converted to nanoaggregates with size 2-20 nm. Random interaction of nanoaggregates forms PDA particles (20-500 nm), which are mainly spherical and tend to aggregate into larger particles (0.5-5  $\mu\text{m}$  in size). Bernsmann et al. (2009) showed that radical compounds and small oligomers are initiators of PDA formation on a substrate. When a dopamine solution is in contact with a surface, monomers in the solution deposit onto the surface through covalent bonding,  $\pi$  stacking, and other noncovalent interactions, resulting in the formation of oligomers and larger molecules on the surface (Fig. 7 b). In other words, large particles and aggregates cannot adhere to a surface without existence of monomers (Jiang et al., 2011).

Due to the covalent and non-covalent bonding capabilities to a broad range of inorganic, organic and metallic substrates, PDA has many potential applications in following fields: antibacterial (Sileika et al., 2011), antifouling (Karkhanechi et al., 2014b), biosensors (Peng et al., 2013), drug delivery vehicles (Cui et al., 2012) and tissue engineering technology (Zhou et al., 2012).

Since its introduction, PDA has attracted substantial interest in membrane modification. PDA is a bio-glue polymer that is easily attached to different substrates. It is proven that PDA grafting to RO membranes can improve antifouling properties and bacterial adhesion resistance of the membranes (McCloskey et al., 2012, Kasemset et al., 2013, Karkhanechi et al., 2014a). In addition, PDA can be

used as an agent for surface functionalization and immobilization due to the presence of many functional groups. Thus, PDA coated membranes could be further modified by other fouling-resistant substances (Karkhanechi et al., 2014b). Overall, PDA offers a new surface modification option with simple steps and reactions for developing high performance membranes (Lee et al., 2007).

**a**



**b**

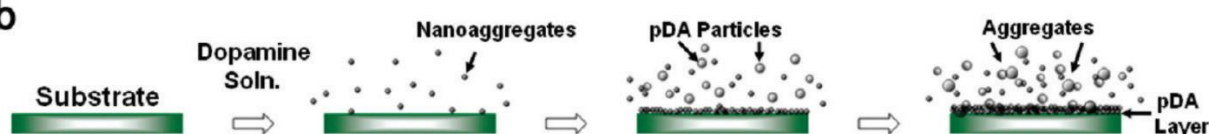


**Fig. 7.** a) Schematic illustration of a possible mechanism of dopamine polymerization (Du et al., 2014). b) Deposition process of PDA on the substrate surface (Jiang et al., 2011)

Generally, the PDA layer causes a hydraulic resistance and decreases membrane permeability (McCloskey et al., 2010). However, there is a competition for water flux between hydrophilicity and the hindrance effect of the extra PDA layer. For example, after coating with PDA for 2 h, 31% water flux decline compared to the virgin membrane was reported, but after further treatment with hydrophilic TiO<sub>2</sub>-NPs, water flux loss was recovered to 14.5% (Zhang et al., 2013).

PEG was grafted onto RO membranes with PDA assistance (McCloskey et al., 2010). Results showed that after 90-min PDA deposition, BSA adhesion to the membranes reduced by 96% at neutral pH. BSA adhesion was further reduced by subsequent PEG grafting onto the PDA-membranes. Similarly, PDA-g-PEG was used to improve the fouling resistance of a pilot-scale test in an RO and UF module as a RO pretreatment (Miller et al., 2013). PDA-UF membranes showed higher permeability, and improved cleaning efficiency compared to the unmodified membrane. Fig. 8 shows the different strategies of dopamine coating in membrane modification.

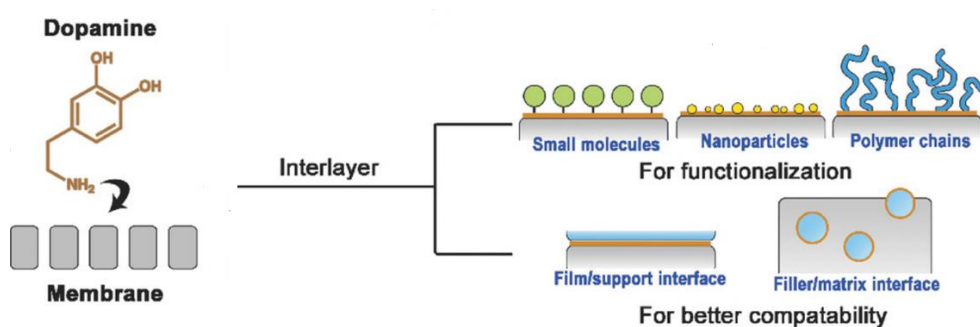


**Fig. 8.** PDA functionality in membrane modification (Yang et al., 2018)

Due to the presence of catechol, PDA can form covalent bonds with amino-terminated reagents through Michael addition or Schiff base reaction (Yang et al., 2018). TOB is a molecule with amine groups which is proved to conjugate with PEG through  $\text{NH}_2$  functional group (Fig. 9) (Du et al., 2015). As a result, it is conceivable that TOB can react with the  $\text{NH}$  group of dopamine. Thus, a mixture of dopamine and TOB, acting as a filler/matrix interface, leads to the conversion of dopamine monomer to PDA which is deposited on the membrane surface while TOB molecules are stuck between PDA particles

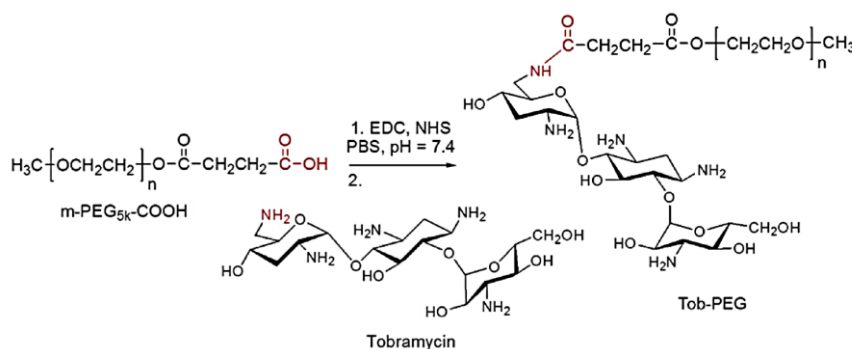


**Fig. 9.** Schematic illustration of the synthesis of polyethylene glycol conjugated tobramycin (Du et al., 2015)



### 3. Experimental

#### 3.1. Materials

Flat-sheet TFC NF membranes were provided by Hangzhou Water Treatment Technology Development Center Co., Ltd, China. Tris (hydroxymethyl) aminomethane, purity  $\geq 99.8\%$ , dopamine hydrochloride, 98% (DA), bovine serum albumin (BSA, Mw  $\sim 67000$ , purity  $> 96\%$ ) and salts were purchased from Sigma Aldrich. Hydrochloric acid (HCl) was purchased from Alfa Aesar. Tobramycin (TOB) 94%, was purchased from Tokyo Chemical Industry Co., Ltd. All the chemicals used in the experiments were in analytical grade.

#### 3.2. Surface modification of TFC membrane

For the preparation of 10 mM Tris buffer solution, first, a 1 M buffer solution was prepared by dissolving 12.1 g tris (hydroxymethyl) aminomethane in 60 ml of DI water and pH of the solution was adjusted to 8.5 by slowly adding 10 % HCl. Then, the volume of the solution was adjusted to 100 ml using deionized (DI) water. To obtain a 10 mM Tris-HCl, a 1:100 diluted solution was prepared from the 1 M Tris-HCl using DI water.

The dopamine solution (2 g/l) was prepared by dissolving 80 mg dopamine hydrochloride powder into 40 ml of Tris buffer solution (10mM, pH 8.5) (Ding et al., 2016).

PDA-membrane was prepared by adding 40 ml fresh dopamine solution (2 g/l) to the membrane surface for a 2-hour coating time (Karkhanechi et al., 2014a). To ensure that only the active layer of the TFC membrane was in contact with the solution, a 10x15 cm virgin membrane was sandwiched between two Teflon frames and fixed tightly with large clips. Before coating, the membrane was soaked in deionized (DI) water for 24 h and then washed thoroughly to remove all substances from the surface and then dried at room temperature.

After adding dopamine into the buffer solution, dopamine starts to polymerize and forms PDA in the alkaline and oxygen condition. This polymerization process occurs at room temperature without stirring, and does not need strict reaction conditions, catalysts or organic solvents.

After the PDA deposition step, the modified membrane (M1) was removed from the frame and

washed thoroughly with DI water. It was then immersed in DI water for 2 h while water was changed several times to remove the weakly-bound PDA from the membrane surface.

The TOB/PDA TFC membrane was prepared by a similar procedure to the PDA-membrane. At the same time, TOB powder was added to the dopamine solution at different concentration (2, 4, and 8 g/l) and then poured on the membrane surface. Fig. 10 illustrates the modified membrane after coating with the TOB/PDA layer.

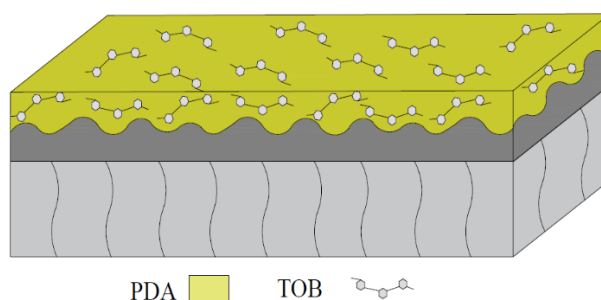


**Fig. 10.** Schematic of TFC membrane surface modification via coating with TOB in PDA matrix

During the polymerization of dopamine in the presence of TOB, it was noticed that TOB may accelerate the polymerization rate since the color of solution containing TOB, changed in a shorter time. As a result, the TOB/PDA membranes (M2, M3, and M4) were prepared by DI water instead of the buffer solution. Modified membranes with different treatments are summarized in Table 1.

The concentration of the dopamine solution (2 g/l) and coating time (2 h) were fixed during modifications (Kasemset et al., 2013).

**Table 1.** Concentration and deposition time of TOB and PDA in different modified membranes

| Membrane | Contact time (h) | TOB (g/l) | Dopamine (g/l) | Buffer solution |
|----------|------------------|-----------|----------------|-----------------|
| M1       | 2                | -         | 2              | Yes             |
| M*2      | 2                | 2         | 2              | Yes             |
| M2       | 2                | 2         | 2              | No              |
| M3       | 2                | 4         | 2              | No              |
| M4       | 2                | 8         | 2              | No              |

### **3.3. Membrane characterization**

Membrane samples were washed with DI water and dried at room temperature for 48 h before characterization.

#### **3.3.1. Water contact angle**

The membrane surface hydrophilicity is typically evaluated by water contact angle measurement. Water contact angles of the membranes were measured using a Kruss Drop Shape Analyzer and DSA4 software with the tangent method. The test for each sample was repeated at least 12 times and the average value was calculated. To have a membrane sample with a flat surface, a 0.5x4 cm sample was cut and stuck to a microscope slide using double sided tape.

#### **3.3.2. Field emission scanning electron microscopy (FESEM)**

FESEM is a type of microscope that produces images with a focused beam of electrons. These electrons are liberated by a field emission source. The object is scanned by electrons according to a zig-zag pattern. FESEM is used to visualize very small topographic details on the surface of an object. In SEM, objects should be conductive. For non-conductive polymeric membranes, surface coating with a thin layer (1.5 - 3.0 nm) of gold or carbon should be performed. During the coating, a carbon source in the form of a rod was mounted in a vacuum system between two high-current electrical terminals. When the carbon source was heated to its evaporation temperature, a fine stream of carbon was deposited onto samples. In this study, surface morphologies of the membranes was observed by FESEM (JEOL JSM 7100F FESEM) after carbon coating in a coater (Quorum Q 150T ES Carbon/Chromium Coater).

#### **3.3.3. Fourier transform infrared (FTIR) spectroscopy**

FTIR spectroscopy is a technique used for obtaining an infrared spectrum of absorption or emission of a solid, liquid or gas. It has been used to detect the changes in structure and composition after chemical modification.

In this study, FTIR was used to analyze the surface chemistry and chemical structures of the virgin and modified membranes between 4000 and 400  $\text{cm}^{-1}$  (Karkhanechi et al., 2014a). It was carried out by a Nicolet 6700 FTIR spectrometer applying attenuated total reflectance (ATR) with diamond crystal. Omnic Spectra software was used to assist with interpretation of data.

### 3.3.4. UV-visible spectroscopy

UV-visible spectroscopy was performed to demonstrate the different absorbance of PDA with and without the buffer solution. The UV-vis. absorbance (300 - 600 nm) of the dopamine solution (2 g/l, in Tris buffer pH 8.5) was measured with a CARY 1bio UV-Visible spectrometer at different time points (2, 10, 20, 30, 45, 60 and 90 min, Tris buffer pH 8.5). The same experiments were carried out using Tris buffer at pH 8.5 and pure water as solvent when TOB (2 g/l) was added to the dopamine solution.

### 3.3.5. Atomic force microscopy (AFM)

Surface roughness of the membranes was analyzed using an AFM (Bruker Innova AFM). AFM enables imaging of the surface features at the atomic level. The AFM images were collected in tapping mode. A silicon tip on a nitride cantilever with a nominal spring constant of 40 Nm<sup>-1</sup> and 300 Hz was scanned at a frequency of 0.5 Hz for a range of 5 µm. The test was repeated four times for each sample and the average data was reported.

## 3.4. Water permeability and salt rejection of membranes

Water flux and salt rejection were evaluated in a lab-scale dead-end cell (HP4750 stirred cell, Sterlitech Corp., USA) with an effective membrane area of 14.6 cm<sup>2</sup>. Membranes were cut into the required shape of the dead-end cell and immersed into DI water before inserting them into the cell. The vessel, filled with 150 ml of solution (pure water or salted water) was pressurized at 20 bar at room temperature (~20.5 °C). Required pressure was provided by a high-pressure nitrogen cylinder equipped with two pressure gauges and pressure was gradually increased.

Water flux (J) was obtained by directly measuring the collected permeate weight (W) for a fixed time (t) in the unit of a liter per square meter per hour (L.m<sup>-2</sup> h<sup>-1</sup>). A balance was connected to a computer and data was collected in an Excel spreadsheet. The balance was set to record the permeate weight every 1 min. By measuring the weight of the steady state flow rate (M), J is calculated by:

$$J = \frac{M}{t \cdot A \cdot \rho}$$

Where  $\rho$  is the density of the permeate water at room temperature, and A is the effective area of the membrane (m<sup>2</sup>).

Salt concentration (mg/l) of the permeate ( $C_p$ ) and feed water ( $C_f$ ) were measured with a conductivity meter, and the salt rejection ( $R$ ) was calculated by the following equation (Choi et al., 2013):

$$R = \left(1 - \frac{C_p}{C_f}\right) \times 100\%$$

Before the salt rejection test, DI water was passed through the membrane for one hour. Then pure water was replaced with salt water and filtration was conducted to produce 10 ml of permeate water. Fig.11 shows a schematic of the setup in which permeate is collected in a beaker and the flux data is recorded by a computer.

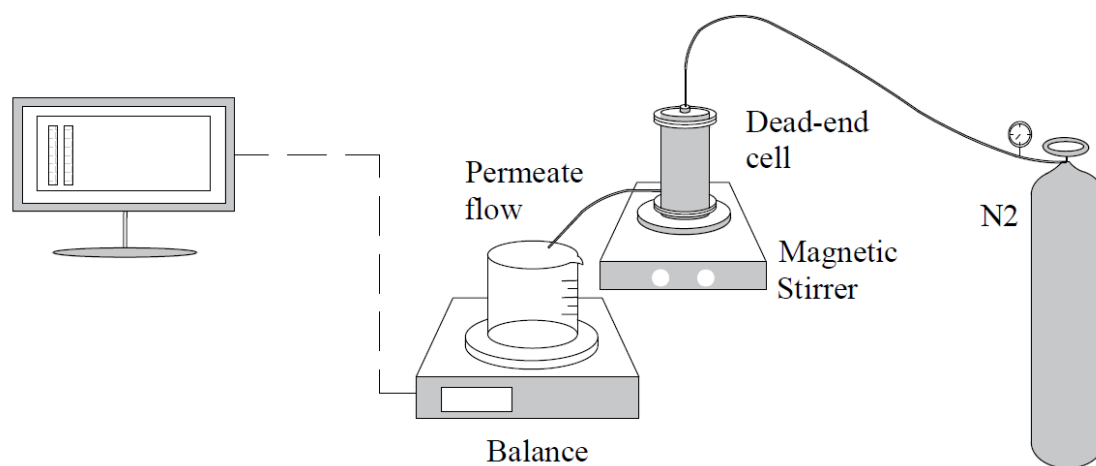


**Fig. 11.** Schematic of the dead-end cell filtration setup.

### 3.5. Organic fouling test

Membrane fouling was evaluated with filtration of a feed solution containing a model organic foulant (BSA) using the high-pressure dead-end cell. A 200 ml BSA (0.5 g/l) solution was filtered for 5 h at 20 bar. The balance was set to record the weight change of permeate every 1 min. The antifouling properties were evaluated by calculating the flux decline ratio (Pan et al., 2016).

### 3.6. Antibacterial test

The anti-bacterial properties of the virgin and modified membranes were investigated by visual monitoring of the bacterial colony growth using disc diffusion test against a typical Gram-negative bacteria *E.coli*. This method is used to show the antibacterial effect of wafers containing antibiotics

on a specific bacteria. If the antibiotics can stop the bacteria from growing, an area where the bacterial growth is inhibited around the samples would be visible. This area is named the inhibition zone and its size indicates the biocidal effectiveness of the antibiotics, which was employed in this study to analyze the antimicrobial properties of the membranes (Pierchala et al., 2018, Kharaghani et al., 2018).

*E.coli* was cultivated on Luria-Bertini (LB) agar plates. LB agar (10 g/l tryptone, 5 g/l yeast extract, 10 g/l NaCl, 50 µg/ml carbenicillin, and 20 g/l agar) solution was autoclaved at 120°C in a wet cycle. Afterward, the LB was left in a water bath (55 °C) to reduce the temperature. The LB media was transferred into plates and the lids were left ajar until the media solidified. An aliquot of *E.coli* (10 µl) from a glycerol stock (50% v/v) was tipped onto each plate and spread with a sterilized loop, followed by placing the round membrane samples (2.5 cm) on the thin layer of bacteria solution from the active side and incubated at 37 °C for 24 h. To better understand the difference between membranes inhibition zones, the test was repeated by splitting each plate evenly to five sections, where each section was imposed by a piece of virgin or modified membrane. All membranes were cut into equal weights and 1 cm in diameter. The test was repeated three times for each membrane. After incubation, the colonies formed around the membrane were examined.

### 3.7. Anti-biofouling Properties

The anti-biofouling properties of virgin and modified membranes were investigated by static adhesion test against *E.coli* bacteria. Bacteria on the membrane surface was monitored by confocal laser scanning microscopy (CLSM, Olympus FluoView FV 1000 IX81).

CLSM is a special type of fluorescent microscopy. In a fluorescent microscope, samples are illuminated with a fluorescent light and then emit a different wavelength of light, where only the fluorescent part of the sample is detectable. In CLSM, images can be obtained at different heights by moving either the sample or the light beam. Biological samples need to be stained with fluorescent dyes to make them visible under the fluorescent light of CLSM.

In this study, all membranes (~1 cm<sup>2</sup>) were first exposed to UV irradiation for 20 min on each side to be sterilized. Then, each membrane was immersed in 2 ml of *E.coli* bacteria suspension in LB broth separately and cultured in a shaking incubator at 37 °C and 70 rpm for two different contacting time (4 and 24 h). To compare the concentration of bacteria solutions, the absorbance of cultures was

measured after 24-h cultivation by a spectrophotometer at OD: 600 nm. Membranes were removed from the bacteria solution after contact time and were immersed in the nutrient medium (LB) to wash the excess bacteria. Afterward, to stain the bacteria, each membrane was removed from the LB broth solution and immersed in a staining solution for 15 min in a dark environment. Staining solution was prepared by dissolving 1.5 µl of each live and dead stain of the BacLight kit into the LB broth solution.

## 4. Results and discussion

In this study, the surface of a commercial TFC membrane was modified by coating a TOB/PDA layer. Since its introduction, PDA has mostly been prepared from the dopamine solution in a buffer solution (pH ~ 8.5) through a pH-induced oxidation. In fact, with the increase in pH, hydrogen protons formed during the oxidation are consumed, and the equilibrium of the reaction shifts toward the product. Thus, kinetics of the reaction is strongly pH-dependent and higher pH is used to manipulate the performance and structure of PDA (Kasemset et al., 2013). However, studies showed dopamine can also be converted into PDA in an acidic solution (pH~ 4) utilizing oxidants such as ammonium persulfate (Wei et al., 2010a). As a result, selection of the oxidants is an alternative to oxygen, and the alkaline condition is not essential. In this study, PDA was formed by dissolving dopamine in DI water in presence of TOB without any added buffer solution where the pH of solution was around 8.5.

It should be noted that although dopamine is soluble in water, PDA is an insoluble substance and the only way to attach it onto the membrane surface is to introduce monomers. As discussed before, PDA coating occurs by the adsorption of monomers and small oligomers on the membrane surface (Ball et al., 2012). Therefore, after dissolving dopamine into the buffer (or TOB) solution, it should be applied on the membrane surface soon.

### 4.1. Membrane characterization

The first characterization of the modified membrane was a visual detection based on the color change of the membrane after modification. Dopamine solution in either TOB or tris buffer started to change in color after 2 min from colorless to light brown. However, the color change occurred in a shorter time for TOB-contained solutions. Fig. 12 shows the color transferring of the dopamine solution above the membrane during the modification process. It is obvious that TOB-dopamine solution becomes darker than the dopamine solution after 1.5 hours. Changing the color of dopamine/TOB solution in DI water instead of tris buffer solution revealed that presence of TOB in the solution is adequate for polymerization of dopamine to PDA. It is believed that alkaline conditions stimulate the oxidation of dopamine (oxidation of catechol to quinone form). Since the pH of the TOB (2 g/l)-dopamine (2 g/l) solution was 8.56, the environment was alkaline and no Tris buffer



solution was needed. To demonstrate the effect of buffer solution, UV-vis spectroscopy was carried out.

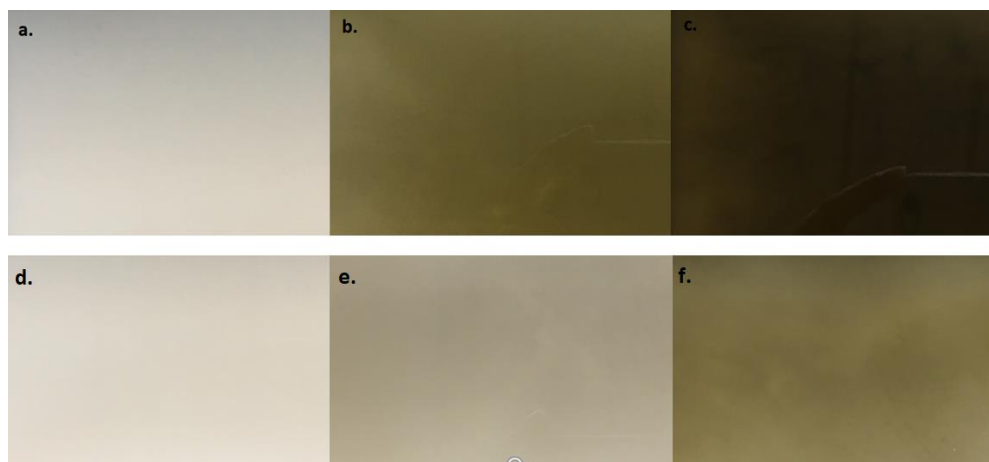


**Fig. 12.** The color of TOB/dopamine (a,b,c) and dopamine (d,e,f) solution in tris buffer solution (pH:8.5) on top of the membrane surface during coating process after 5min, 45 min, and 90min from left to right

After deposition of PDA with different concentrations of TOB, the color of the modified membranes differed where higher TOB concentrations resulted in darker modified membranes. For example, after washing the residue solution, the color of the modified membrane M3 was darker than M2 and M1, probably because a thicker layer of PDA was coated on the membrane surface.

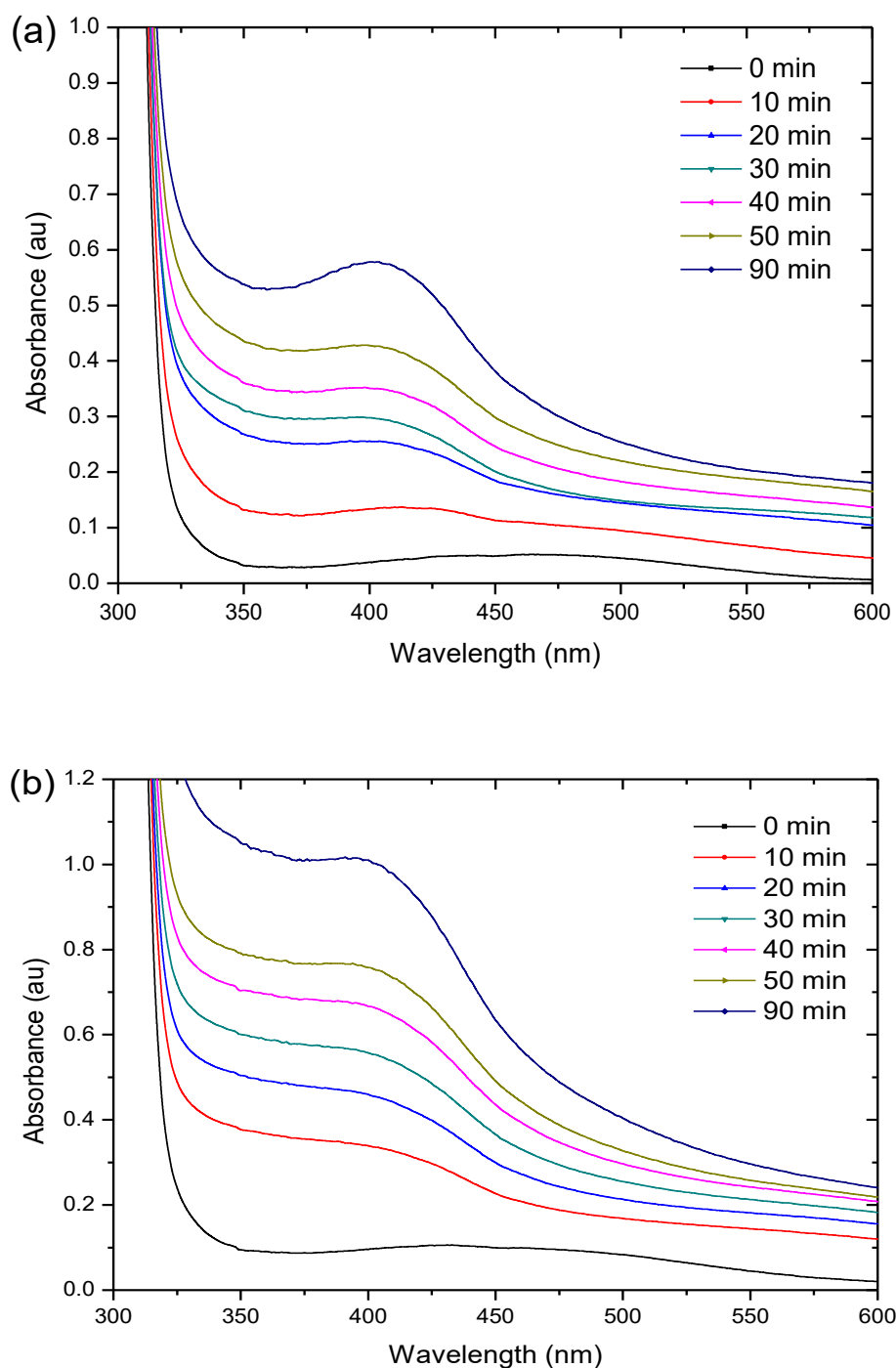
#### 4.1.1. Dopamine reactivity

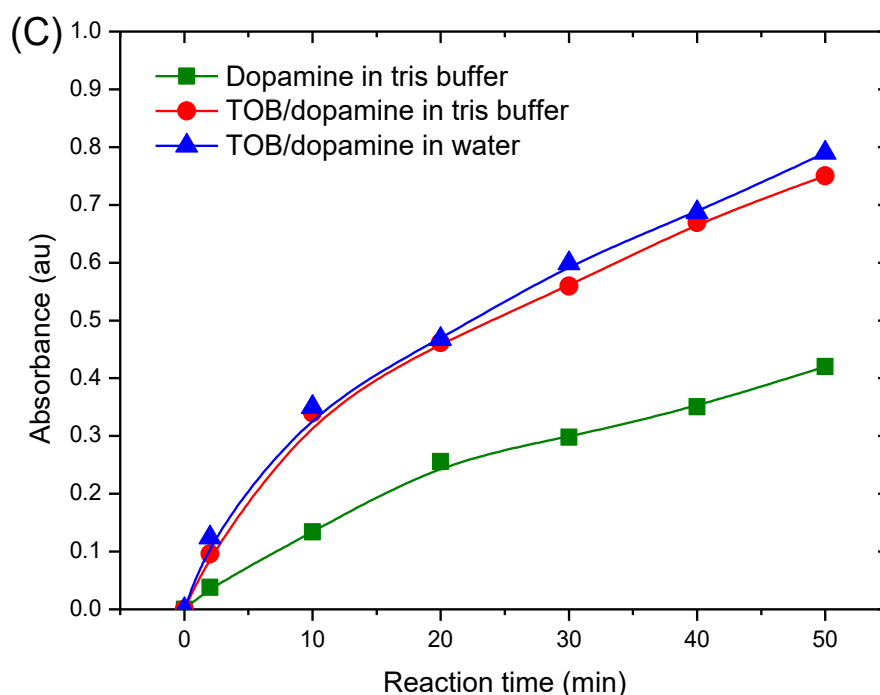
The reactivity of the dopamine and TOB/dopamine in the buffer solution and DI water was measured at room temperature by UV-vis spectroscopy. To understand the polymerization reaction over time, the measurement was carried out every 10 min.

Fig. 13 shows the UV-vis spectra of dopamine solution (2 g/l in Tris (pH~8.5)) during the oxidation reaction with and without TOB. Absorption intensity increased with time and a broad peak at 400 nm was obvious after 90 min assigning to the  $C=C-C=O$  structure of the quinone (Yang et al., 2016, Cheng et al., 2012). This is in agreement with the polymerization reaction where the catechol groups oxidize into quinone and the subsequent polymerization.

Fig. 13c compares the absorption intensity by dopamine and TOB/dopamine in either buffer solution or water at 400 nm over reaction time. The absorption intensity of all solutions increased with time indicating polymerization proceeds by time (Wei et al., 2010a) either with or without buffer

solution. Moreover, the absorption intensity of the TOB/dopamine in the buffer solution and water was almost the same at different running time. This indicates that, reactivity of dopamine in presence of TOB is independent of the buffer solution. In other words, since the dopamine/TOB was an alkaline solution with pH  $\sim 8.5$ , the tris buffer solution is not required for the polymerization. It is also noticeable that the absorption intensity of the dopamine/buffer solution without TOB was lower than that of the dopamine/buffer solution with TOB revealing that TOB accelerates the reaction rate of dopamine polymerization.





**Fig. 13.** UV-vis spectra of (a) dopamine (2 g/l) in Tris (pH: 8.5), (b) TOB (2 g/l) + dopamine (2 g/l) in Tris (pH: 8.5), and (c) Time dependent absorbance of dopamine solutions at 400 nm

#### 4.1.2. Morphology analysis

The morphologies of the virgin and modified membrane were observed by FESEM and the roughness were measured by AFM.

Fig. 14 shows the surface structures of the modified and virgin membranes. All membranes had a “leaf-like” and uniform structure on the surface (Wang et al., 2017) and no considerable difference can be seen between the modified (except M4) and virgin membranes. This reveals that a very thin layer of PDA is deposited on the membrane surface. Also, no difference was observed between the surfaces of the modified membrane with and without buffer solution. In addition, PDA is deposited without any visible agglomeration for M1, M2 and M3, but aggregation of PDA is visible when the concentration of TOB is increased (Karkhanechi et al., 2014a). Higher TOB content in the dopamine solution resulted in the formation of larger PDA particles in a shorter time and thus agglomeration of PDA on the membrane surface. As a result, the round PDA particles (0.5μm in diameter) can be seen on the modified membrane M4.

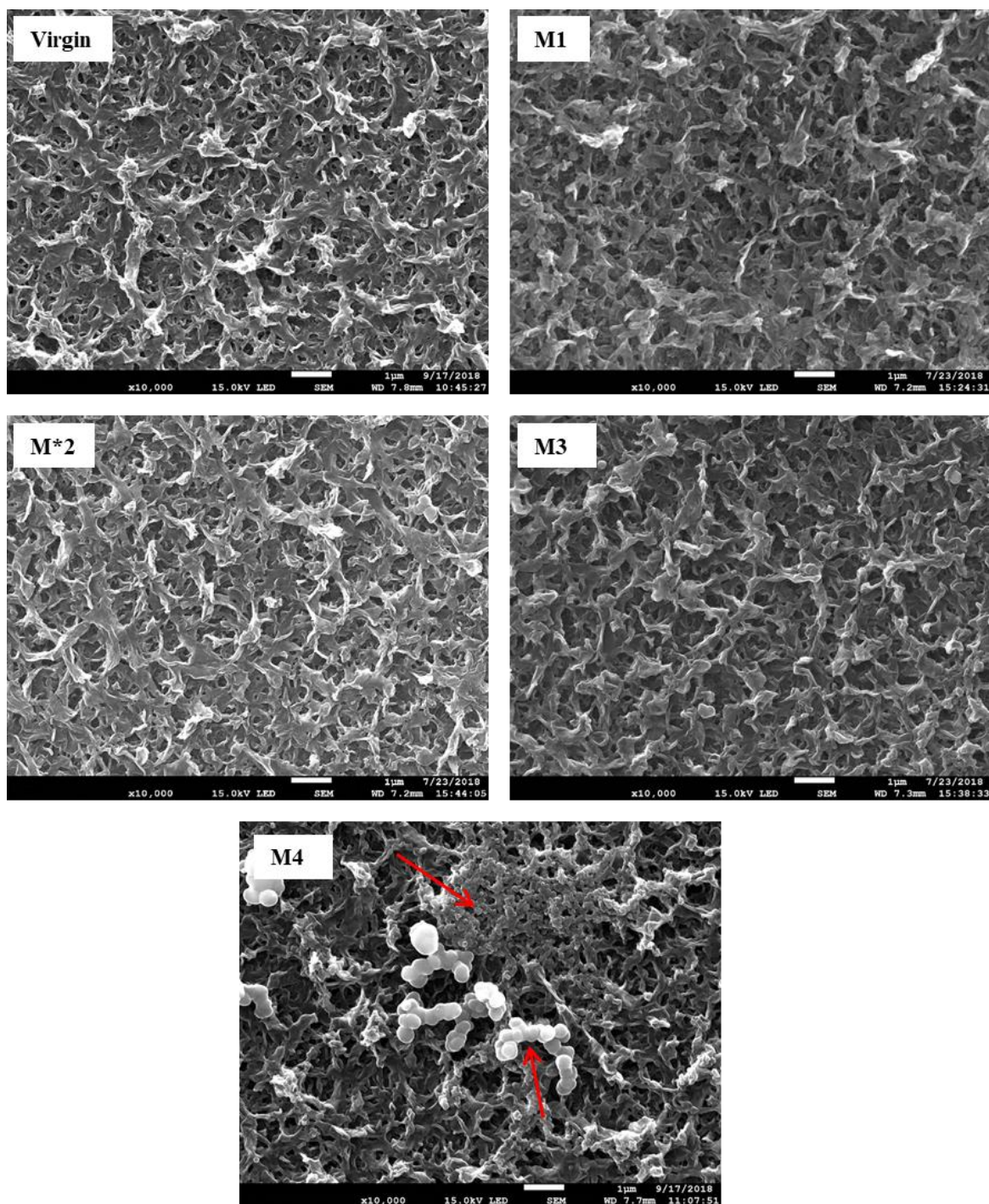


**Fig. 14.** FESEM images of the virgin and modified membranes (M1, M\*2, M3, and M4)

The roughness parameters of the modified and virgin membranes were measured on a  $25 \mu\text{m}^2$  of each sample for four times. Fig. 15 shows the average values of  $R_a$  and  $R_q$  for all membranes considering the standard deviation parameter as the error bar. It is obvious that the membrane roughness increased after modification for all membranes due to the PDA layer on the membrane surface. TOB had a minor effect on surface roughness. The modified membrane M3 showed a slightly smoother surface compared with the other modified membranes. It is predicted that the concentration

of TOB in the solution affected on the size of the PDA particles in the membrane surface coating.

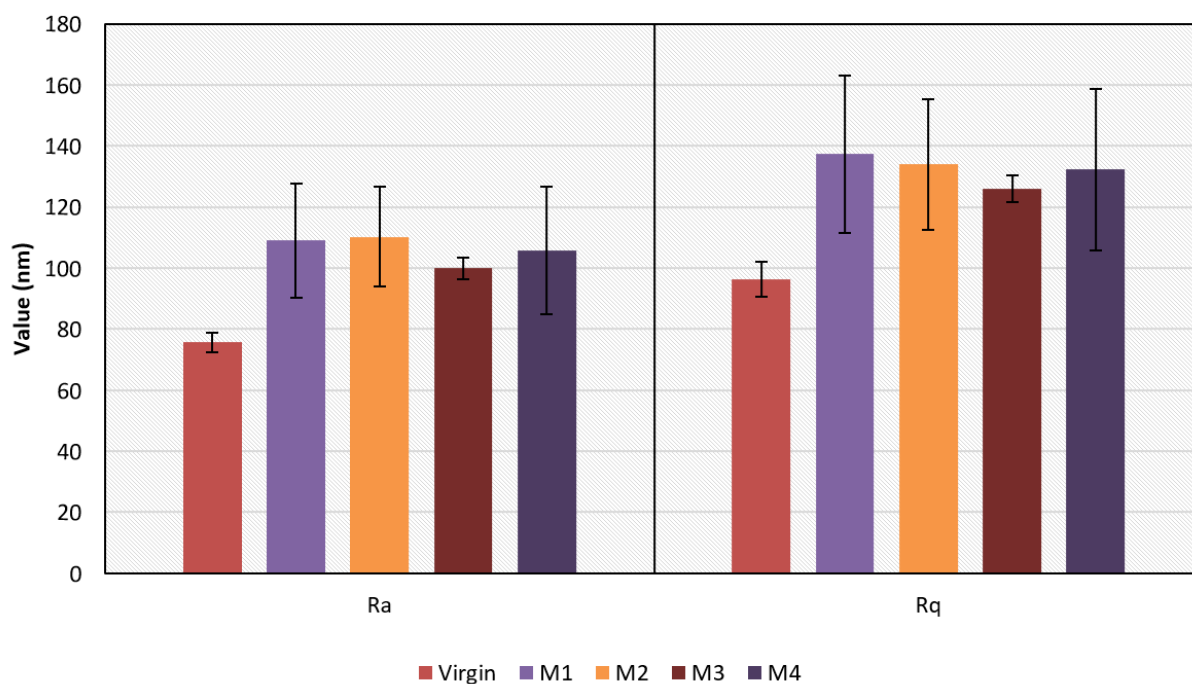








**Fig. 15.** Roughness parameters for the virgin and modified membranes. Rq represents the root mean square and Ra is the average roughness.

#### 4.1.3. Surface hydrophilicity

Hydrophilicity of the membrane surface is usually evaluated by water contact angle measurement. Table 2 presents the static water contact angles of the modified and virgin TFC membranes. All the modified and virgin membranes showed hydrophilic surfaces as their water contact angles were below  $90^\circ$ . PDA coating can improve the hydrophilicity of the membrane surface due to the hydroxyl, catechol and amine groups (Liao et al., 2010). In this research the PDA modified membrane (M1) showed a water contact angle of  $31^\circ$ , which was reduced by 40% compared to that of the virgin membrane M0 ( $51^\circ$ ). However, the TOB treated membranes (M\*2, M2 and M3) had even lower water contact angles ( $< 25^\circ$ ), which were less than half of the water contact angle of the virgin membrane. Using higher concentration of TOB (8 g/l) for the modified membrane M4, resulted in higher contact angle ( $34^\circ$ ) compared to the other modified membranes. It suggests that TOB can significantly affect the surface hydrophilicity of the membrane due to the influence on the PDA particles size. As shown by the SEM images in Fig. 14, high concentration of TOB (8 g/l) resulted in larger and agglomerated PDA particles.

**Table 2.** Water contact angles of the virgin and modified TFC membranes

| Membrane |            | Water contact angle (deg.)   |
|----------|------------|--|
| M0       | $51 \pm 2$ |  |
| M1       | $31 \pm 5$ |  |
| M*2      | $25 \pm 3$ |  |
| M2       | $25 \pm 3$ |  |
| M3       | $20 \pm 1$ |  |
| M4       | $34 \pm 2$ |  |

Interestingly, the TOB/PDA modified membranes with and without the buffer solution (M\*2 and M2) showed almost the same water contact angle ( $25^\circ$ ), suggesting the buffer solution is not required when TOB is applied with dopamine as it is sufficient to facilitate the polymerization of dopamine.

#### 4.1.4. Analysis of membrane chemical structure

The FTIR spectra of the modified and virgin membranes in the range of  $400\text{--}1800\text{ cm}^{-1}$  are presented in Fig. 16. The characteristic peaks of the TFC membrane were revealed by the spectrum of the virgin membrane, where the peak at  $1509\text{ cm}^{-1}$  represents N-H bending (Yang et al., 2014, Wang et al., 2018) and the peak at  $1712\text{ cm}^{-1}$  shows the stretching of the C=O bond of the neat membrane (Uddin et al., 2006, Choi et al., 2013). Peaks at  $2970$  and  $1340\text{ cm}^{-1}$  corresponded to the saturated C-H stretching and bending. The absorption of C=C bond of the aromatic compound probably appeared at  $1590\text{ cm}^{-1}$ , and the small peak at  $1614\text{ cm}^{-1}$  corresponds to the C=N (Choi et al., 2013).



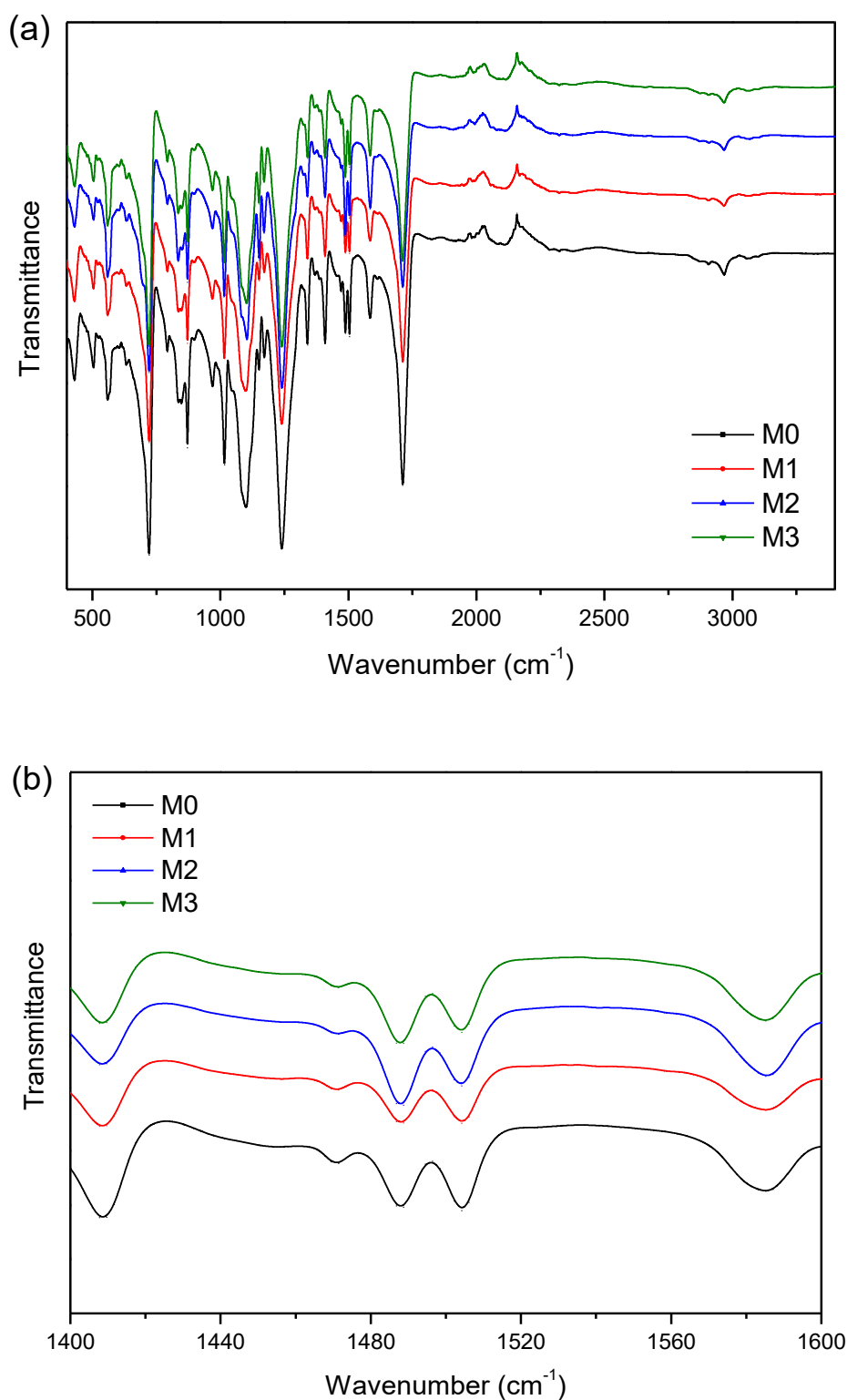


**Fig. 16.** FT-IR spectra of the virgin and modified membranes in the range of a) 400-3400  $\text{cm}^{-1}$ , b) 1400-1600  $\text{cm}^{-1}$

The broad peak at 1100  $\text{cm}^{-1}$  represents C-O or C-N bond stretching and peak at 1240  $\text{cm}^{-1}$  belongs to the C-O vibration of phenolic moieties (Müller and Keßler, 2011). The virgin and modified membranes demonstrated little difference in chemical structures since the functional groups

in PDA and TOB are almost the same as those in the TFC virgin membrane (Hegab et al., 2016). Furthermore, since the surface modification occurred on the very thin skin layer of the membrane, the intensity of the peaks did not change significantly due to the small amount of TOB and PDA molecules on the membrane surface.

However, Muller et al, (2011) reported that peaks at 1490, 1435, 1250  $\text{cm}^{-1}$  evolved in dopamine solution in the tris buffer (pH 8.5) after 2 h corresponding to the dopamine reaction products including PDA. As a result, increase of the intensity of the peak at 1490  $\text{cm}^{-1}$  is expected comparing to the peak at 1504  $\text{cm}^{-1}$  for the modified membrane belongs to the PDA layer on the membrane surface (Fig. 16 b).

#### **4.2. Membrane permeability and salt rejection**

The water permeability and salt rejection of the virgin and modified membranes were measured by a dead-end cell at 20 bar. Table 3 presents the pure water permeability ( $\text{L}/\text{m}^2\cdot\text{h}\cdot\text{bar}$ ) and  $\text{Na}_2\text{SO}_4$  and  $\text{NaCl}$  salt rejection for the virgin and modified membranes. Results showed that water permeability declined from 1.60 ( $\text{L}/\text{m}^2\cdot\text{h}\cdot\text{bar}$ ) for the virgin membrane to 1.14 ( $\text{L}/\text{m}^2\cdot\text{h}\cdot\text{bar}$ ) for the modified membrane M3 due to the hydraulic resistance of the PDA layer (Wang et al., 2018, Karkhanechi et al., 2014a). It should be noted that hydrophilicity and diffusion resistance are two main factors for permeability of TFC membranes. As a result, although hydrophilicity of the modified membranes has improved, the mass transfer resistance of the PDA layer can result in lower flux (Karkhanechi et al., 2014a). In addition, the modified membrane M3 showed the lowest water permeability due to the thicker PDA layer on the membrane surface.

Considering the errors of the measurements, salt rejections of the virgin and modified membranes were similar, at around 70% for  $\text{NaCl}$  and 76% for  $\text{Na}_2\text{SO}_4$ . Since salt rejection is governed by the active layer of the TFC membrane, unchanged rejection performance suggests that our modification did not damage membranes (Karkhanechi et al., 2014b). However, the slight increase of salt rejection represented the effect of the PDA layer on the membrane surface.  $\text{Na}_2\text{SO}_4$  rejections of the membranes were higher than those with  $\text{NaCl}$ , which confirms that membrane rejection to multivalent ions is higher than that to monovalent ions. It should be noticed that the measurement of salt rejection by the dead-end cell may have some errors due to the high concentration



polarization near the membrane surface (McCloskey et al., 2010). The salt rejection of the membrane may vary with the volume of the collected permeate.

**Table3.** Water fluxes and salt rejections of the virgin and modified membranes

| Membrane                                      | Virgin      | M1          | M*2         | M2          | M3          |
|---|-------------|-------------|-------------|-------------|-------------|
| Water flux (L/m <sup>2</sup> h. bar)          | 1.60 ± 0.12 | 1.24 ± 0.10 | 1.23 ± 0.10 | 1.24 ± 0.09 | 1.14 ± 0.10 |
| NaCl Rejection (%)                            | 70.0 ± 2.5  | 69.0 ± 3.0  | 69.0 ± 2.5  | 70.0 ± 2.4  | 71.0 ± 3.2  |
| Na <sub>2</sub> SO <sub>4</sub> Rejection (%) | 75.8 ± 1.5  | 76.0 ± 2.5  | 76.0 ± 2.5  | 76.0 ± 2.1  | 77.0 ± 1.0  |

### 4.3. Organic fouling evaluation

Fig. 17 shows the normalized flux change of the modified and virgin membrane as a function of BSA (0.5 g/l) filtration time. The permeation flux reduced with time for all membranes due to membrane fouling. To exclude the impact of ion concentration polarization on the water flux decline, we selected the BSA solution without any salt. Obviously, flux decline of the virgin membrane was up to 80% after 320-min filtration. All the modified membranes showed much less flux decline, suggesting the significantly improved organic fouling resistance of the membrane. In particular, the modified membrane M3 exhibited the best antifouling performance. After 320-min BSA filtration, the water flux of M3 was still 72%, more than 3 times higher than that of the virgin membrane (20%). The excellent antifouling performance of M3 agreed well with its lowest water contact angle (Table 2).

The improved flux performance during BSA filtration is attributed to the antifouling properties explained by the improved hydrophilicity of the membrane surface after modification. Although PDA and TOB modification slightly reduced the water permeability of the membrane, it endowed strong antifouling properties to the modified membranes. In real applications, feed solution is saline water containing a high amount of hydrophobic matters, such as proteins and bacteria. As a result, a hydrophilic surface can significantly prevent the attachment of these foulants by forming a hydration layer near the membrane surface.

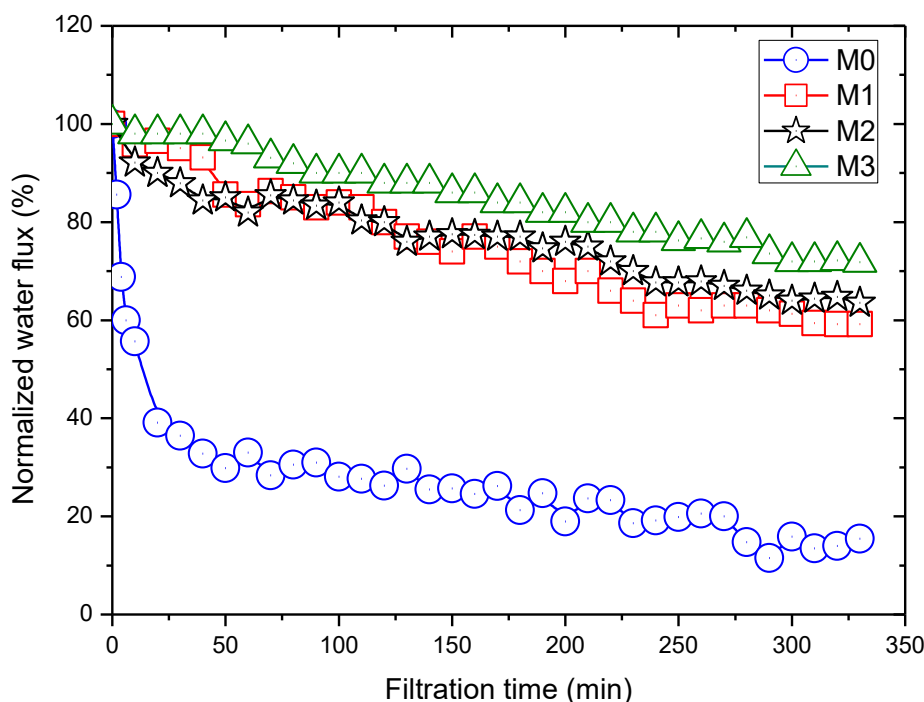


**Fig. 17.** Normalized flux change of the virgin and modified membranes with time during the filtration of BSA (0.5 g/l). The initial fluxes for virgin, M1, M2 and M3 were 32, 24.8, 24.8 and 22.4 (LMH) respectively.

In the long-term operation (after 150 min), the TOB modified membrane (M2) showed slightly higher water flux than the PDA modified membrane (M1), suggesting better antifouling performance of the membrane modified by TOB, although such improvement was not obvious in the beginning of the filtration (before 150 min). However, as an antibiotic, TOB is expected to significantly improve anti-biofouling properties of the membrane, and the results are displayed in the next section.

#### 4.4. Anti-biofouling properties

Generally, the anti-biofouling property of the membrane can be achieved by active and passive strategies (Sileika et al., 2011). The passive strategy refers to the inhibition of bacteria from attaching to the membrane surface through the antibacterial coating layer. For example, the PDA modified membranes exhibited remarkably enhanced antibacterial activities (Su et al., 2016). It is believed that, the mechanism of cell death is the damage of cell walls when the bacteria contact to the PDA coating on the membrane surface. The increased surface roughness is the main reason for antibacterial properties. SEM images of cells revealed that, the bacteria treated with high roughness PDA coatings was shrunk and lost its spherical shape indicating possible damage to the cell membrane.

Another example of passive strategy is the incorporation of GO into TFC membrane to improve the antimicrobial properties due to the both physical and chemical interactions between the GO and the bacteria (He et al., 2015). The sharp edges of GO nano-sheets is believed as the main reason of cell damaging. SEM images proved that the direct contacts of graphene nano-sheets with cells leads to disturbing them. Although the passive strategy is strongly applicable, it shows restriction confronting bacteria proliferation.

In contrast, the active strategy refers to the promoting bacteria killing through the release of the active agent by interfering with biochemical pathway. Studies suggest that materials smaller in size, such as nanoparticles have higher cytotoxicity than those with larger sizes (Liu et al., 2011). In this regard, nanoparticles, such as silver, have antibacterial properties due to the release of Ag ions as well as direct contact-killing mechanisms (Kharaghani et al., 2018). As a result, silver nanoparticles embedded in a polymeric matrix exhibit a strong antibacterial properties. The inhibition zone surrounding the chitosan membranes embedded with silver ions and nanoparticles against the *E.coli* bacteria was observed (Zhu et al., 2010).

In this study, the anti-biofouling properties of the modified membranes were investigated by the disc diffusion method against *E.coli* bacteria. This method is an effective technique to understand the antibacterial properties of those biocides which act through the active strategy. Tobramycin first crosses the bacterial membrane and works by binding to the ribosome and results in cell death due to the prevention of protein formation (Haddad et al., 2002).

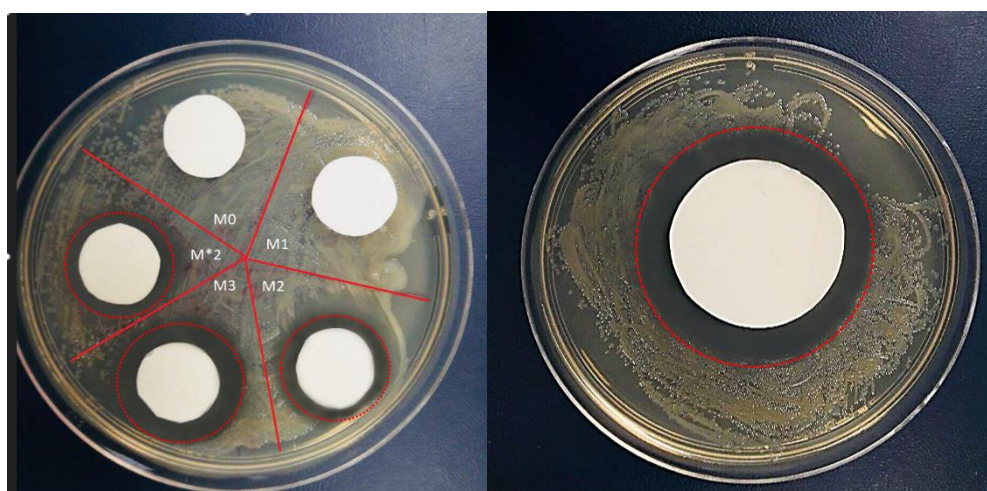


**Fig. 18.** Visual images of the inhibition zone against *E.coli* bacteria indicated by red dotted circle for virgin and modified membranes (left) M3 modified membrane (right)

Fig. 18 presents the inhibition zones of the virgin and modified membranes. TOB modified membrane (M2, M\*2, and M3) showed a strong antibacterial activity against *E.coli* bacteria. In contrast, no inhibition zone was observed for the PDA-modified membrane (M1) and the virgin membrane. These results indicate that the antibacterial properties of the modified membranes (M2 and M3) come from TOB on the membrane surface. Both TOB and PDA, have proven antibacterial properties according to the previous studies (Wang et al., 2018, Karkhanechi et al., 2014a). However, since TOB is the only substance that can be released to the aqueous environment, no inhibition zone was observed for the PDA modified membrane (M1) in the disc diffusion method. Notably, the diameter of the inhibition zone of M3 was larger than that of M2, since M3 was modified by TOB with a higher concentration (4 g/l).

The anti-biofouling properties of the virgin and modified membranes were also evaluated by static adhesion of *E.coli* bacteria by immersing membrane coupons into the bacteria solution for 4 and 24 h. Instead of washing membranes with water or NaCl solution for several times, the membranes were gently washed only once by the same LB broth to observe all the absorbed bacteria on the membrane surface.

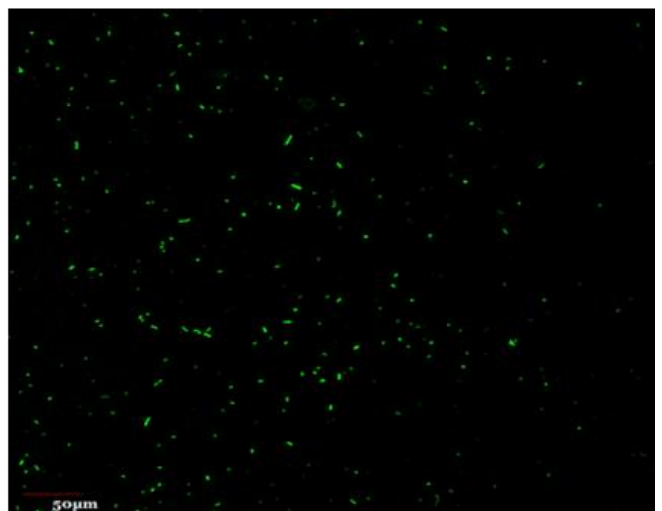
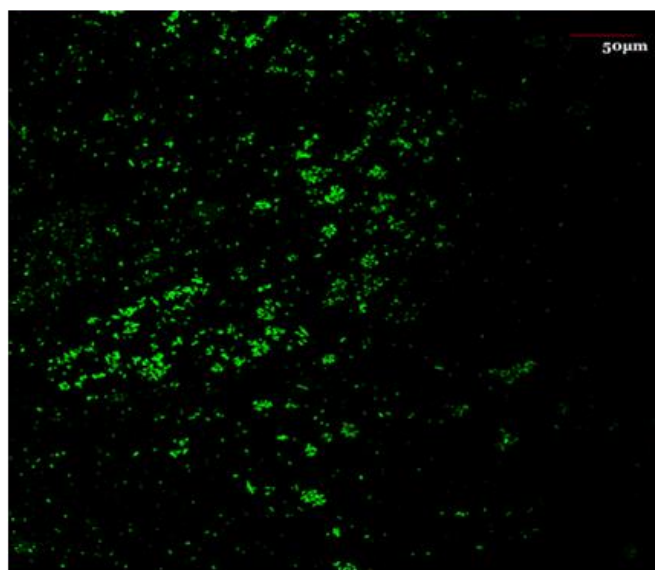
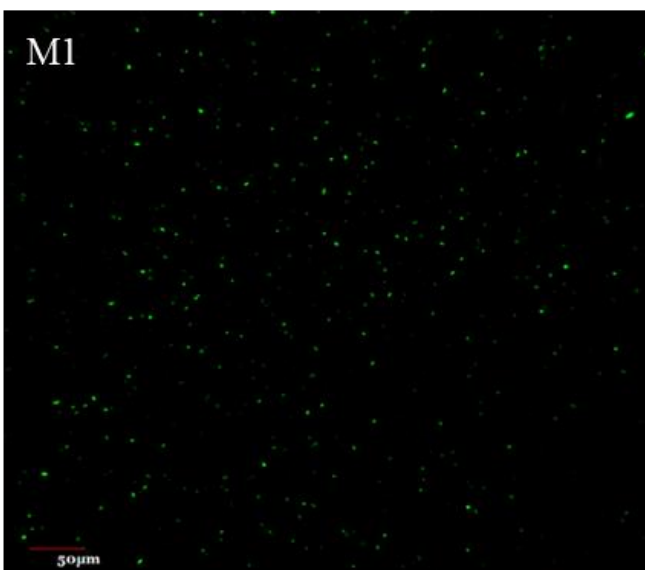
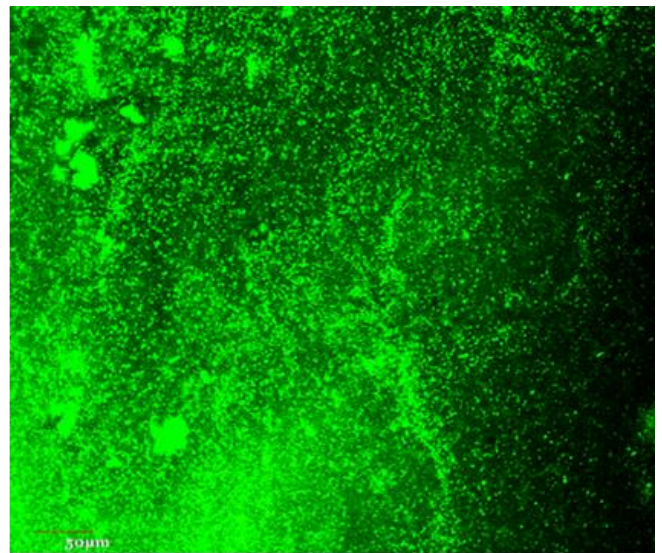
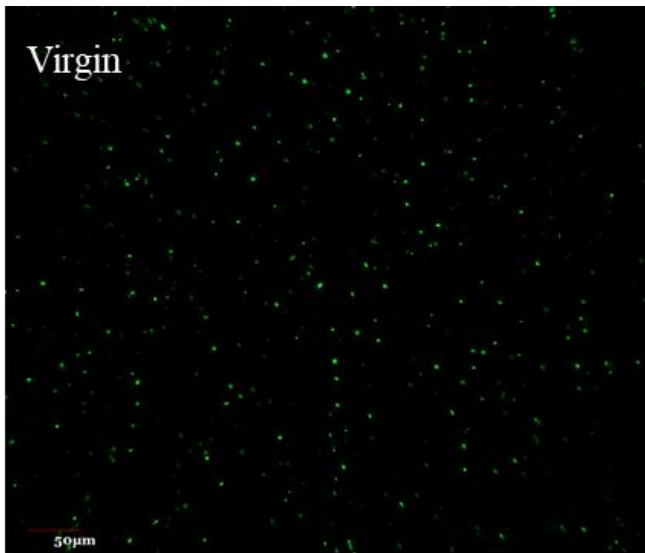
To understand the long term effect of modified membrane, the static adhesion test was performed for the membrane M3 after 6-h filtration of NaCl and BSA solutions defined by M3-used.

The cell concentration from the optical density (OD<sub>600</sub>) by a spectrophotometer is shown in Table 4. Using the following formula, the bacteria concentration was estimated  $\sim 2 \times 10^9$  cell/ml for different samples after 24-h cultivation. This predicts consistent condition for different samples.

$$\text{OD}_{600} \text{ of } 1.0 = 8 \times 10^8 \text{ cells/ml}$$

**Table 4.** Absorbance of the cultivated bacteria solution for different membrane samples

| Membrane | Abs. OD 600 nm |
|----------|----------------|
| M0       | 2.7 ± 0.1      |
| M1       | 2.9 ± 0.1      |
| M2       | 2.5 ± 0.1      |
| M3       | 2.9 ± 0.1      |
| M4       | 2.6 ± 0.1      |
| M2-used  | 3.0 ± 0.1      |



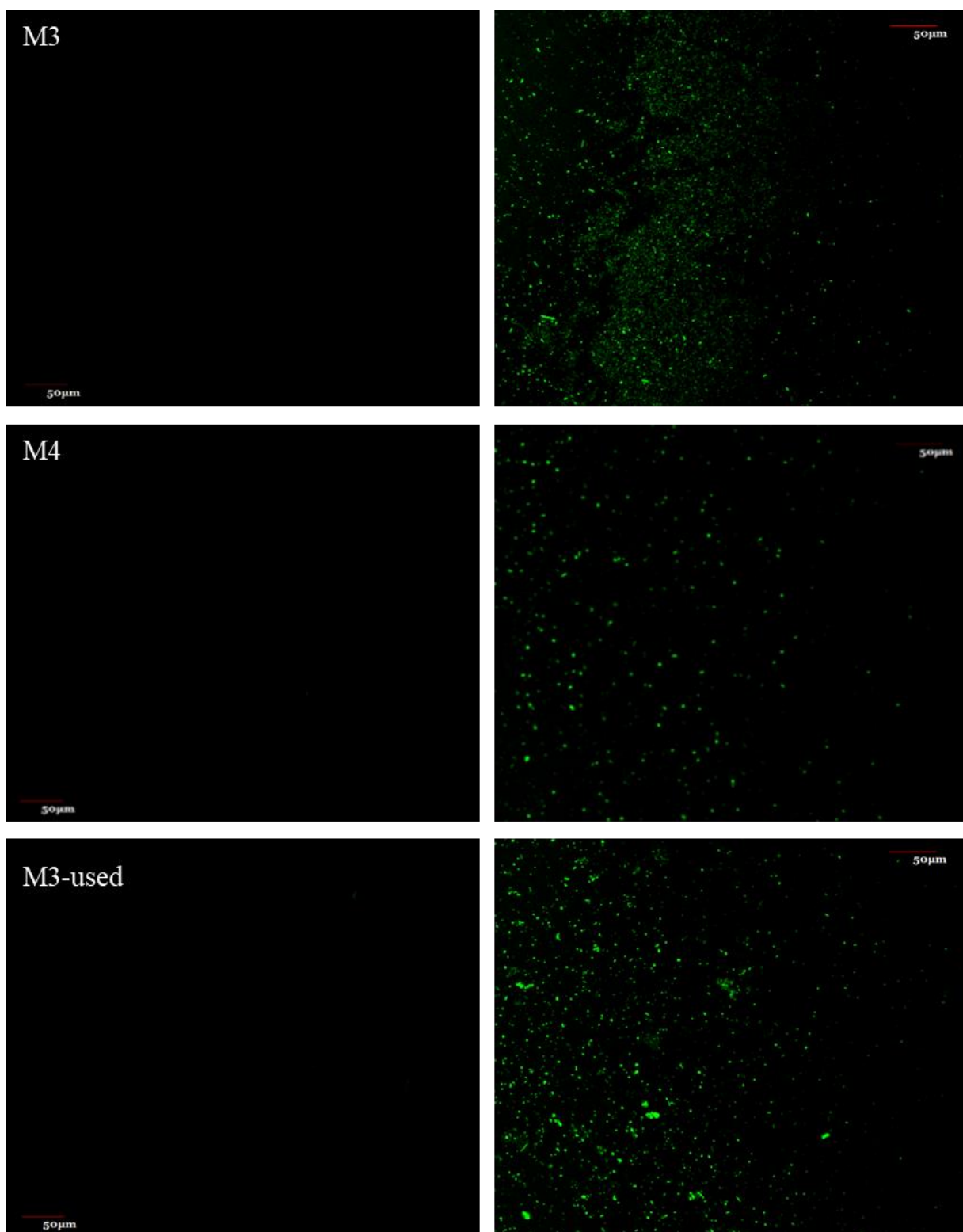


**Fig. 19.** CLSM images of *E.coli* on the virgin and modified membranes after 4 h (left) and 24 h (right) cultivation, the black background is the membrane surface and green points are stained bacteria

Fig. 19 presents the images of confocal microscopy for the virgin, modified, and used modified membranes after cultivation. It is noticeable that all modified membranes have the anti-biofouling properties comparing to the virgin membrane. After 24 h, a huge number of bacteria attached on the

virgin membrane surface while this amount is countable for modified membranes. M2 and M4 showed the better result than the M3 modified membrane which might be a result of the higher concentration of M3 bacteria solution (Table 4). Also, no dead bacteria were seen on the modified membrane surface after 24 h. The attachment of dead bacteria is also considered as a problem since it cannot be removed from the surface and increase the biofilm thickness.

It can also be observed that after 4 h, no bacteria were attached on the modified membrane with TOB (M2, M3, and M4). It can be explained by the minimum inhibitory concentration (MIC) of TOB and low concentration of bacteria. MIC is the lowest concentration of a biocide which prevents the growth of bacteria. As a result, after 4-h incubation, the concentration of TOB around the membrane surface was equal or higher than MIC where no bacteria growth was seen on the surface of modified membranes. This effect is apparent since no antibacterial effect was seen on the PDA modified membrane (M1). The biocidal effect of TOB on the membrane surface clearly decreased after 24 h cultivation, due to the increasing the concentration of bacteria.

Comparing the PDA modified membrane and virgin membrane after 24-h cultivation revealed an antibacterial property for the modified membrane M1. Studies showed that the PDA modified membrane inhibited the bacteria growth on the membrane surface due to the passive antibacterial properties (Karkhanechi et al., 2014b). The anti-biofouling properties of PDA modified membrane (M1) are attributed to the bactericidal property of protonated amine group in PDA (Karkhanechi et al., 2014a).

Results also show an antibacterial property of the membrane M3-used. No bacteria attachment after 4-h cultivation and slightly increased number of bacteria compared to the membrane M3 after 24-h cultivation can be seen. This shows that after 6-h contact with water, the antibacterial properties remain in the modified membrane but are slightly reduced due to the release of TOB to the water.

It should be noted that TOB molecules cannot pass through the TFC membrane and enter the permeate flow. In another word, if TOB was released from the membrane surface to water during the filtration process, it would be conducted to the municipal sewage channels or wastewater basins for further treatment through the concentrate flow of RO or NF membranes.



## 5. Conclusion

A commercial TFC membrane was successfully modified by TOB immobilization to improve its antifouling properties. A “bio-glue” polydopamine (PDA) was applied to immobilize the antibiotic onto the membrane surface. PDA acts as a matrix which attached TOB on the membrane surface during its self-polymerization.

The deposition of PDA was verified by visual observation and water contact angle tests. The hydrophilicity of the modified membrane was significantly improved due to the PDA coating. As a new finding of this study, UV-vis absorbance of the dopamine/TOB solution in contact with water and Tris buffer solution revealed that using TOB, dopamine polymerization can take place without any buffer solution. SEM images of the modified membranes showed that concentration of TOB affects the formation of PDA particles. Among all modified membranes, the higher concentration of TOB (8 g/l) showed the 0.5- $\mu$ m spherical PDA particles while no PDA aggregation was observed with other TOB concentrations.

The salt rejection of the membrane was not affected by PDA or PDA/TOB coating demonstrating that the coating did not damage the active layer. However, the water permeability slightly decreased due to the extra resistance of the PDA layer. The modified membranes showed 30% flux decline after 320-min filtration of BSA (0.5 g/l) while this value was 80% for the virgin membrane. Although water fluxes of the modified membranes reduced, they showed better antifouling performance against organic foulant BSA over time due to the improved hydrophilicity.

The inhibition zone around the TOB modified membranes in the disc diffusion test demonstrated the active antimicrobial properties of the membranes due to the release of TOB. In contrast, in the static adhesion test, all modified membranes showed anti-biofouling properties against *E.coli* bacteria attachments. CLSM images showed far less live bacteria on the membrane surface after 24-h cultivation for modified membranes, which could be contributed to the passive antimicrobial properties of PDA and TOB on the surface. However, only TOB modified membranes revealed antibacterial properties after 4-h cultivation. This can be introduced by the active antifouling due to the low bacteria concentration around the surface.



The study also revealed recommendations for future work, as listed below:

TOB can also be applied on the surface of the PDA coated membrane instead of mixing with the dopamine solution. Due to the functional group of PDA, TOB molecules can be attached to the surface which might improve the antibacterial properties of modified membranes. Moreover, roughness and surface charge might be changed which can alter the protein fouling.

PDA modified membranes showed a rough structure similar to the virgin membrane. To achieve a smoother surface, polyethyleneimine (PEI) can be added to the dopamine solution (Zhang et al., 2014). Effects of the reduced roughness using PEI could reduce protein and bacteria attachments, leading to better antifouling performance.

To reduce the mass transfer resistance of the PDA layer, other parameters such as deposition time and dopamine concentration should be further optimized. Reducing deposition time will decrease the PDA layer thickness, but might affect the attachment of TOB molecules onto the membrane surface.

Last but not least, studying the long-term antimicrobial properties of the modified membranes is required. In this study, long-term antimicrobial performance was not investigated due to the restricted time of research. However, the modified membranes should have long-term stable antifouling properties over time.

## Reference

- ABDELRASOUL, A., DOAN, H. & LOHI, A. 2013. Fouling in Membrane Filtration and Remediation Methods.
- ALI, M. E. A., WANG, L., WANG, X. & FENG, X. 2016. Thin film composite membranes embedded with graphene oxide for water desalination. *Desalination*, 386, 67-76.
- ASADOLLAHI, M., BASTANI, D. & MUSAVI, S. A. 2017. Enhancement of surface properties and performance of reverse osmosis membranes after surface modification: A review. *Desalination*, 420, 330-383.
- AZARI, S. & ZOU, L. 2012. Using zwitterionic amino acid l-DOPA to modify the surface of thin film composite polyamide reverse osmosis membranes to increase their fouling resistance. *Journal of Membrane Science*, 401-402, 68-75.
- AZARI, S. & ZOU, L. 2013. Fouling resistant zwitterionic surface modification of reverse osmosis membranes using amino acid l-cysteine. *Desalination*, 324, 79-86.
- BALL, V., FRARI, D. D., TONIAZZO, V. & RUCH, D. 2012. Kinetics of polydopamine film deposition as a function of pH and dopamine concentration: Insights in the polydopamine deposition mechanism. *Journal of Colloid and Interface Science*, 386, 366-372.
- BELFER, S., GILRON, J., PURINSON, Y., FAINSHTEIN, R., DALTROPHE, N., PRIEL, M., TENZER, B. & TOMA, A. 2001. Effect of surface modification in preventing fouling of commercial SWRO membranes at the Eilat seawater desalination pilot plant. *Desalination*, 139, 169-176.
- BELFER, S., PURINSON, Y., FAINSHTEIN, R., RADCHENKO, Y. & KEDEM, O. 1998. Surface modification of commercial composite polyamide reverse osmosis membranes. *Journal of Membrane Science*, 139, 175-181.
- BEN-SASSON, M., LU, X., BAR-ZEEV, E., ZODROW, K. R., NEJATI, S., QI, G., GIANNELIS, E. P. & ELIMELECH, M. 2014a. In situ formation of silver nanoparticles on thin-film composite reverse osmosis membranes for biofouling mitigation. *Water Res*, 62, 260-70.
- BEN-SASSON, M., LU, X., NEJATI, S., JARAMILLO, H. & ELIMELECH, M. 2016. In situ surface functionalization of reverse osmosis membranes with biocidal copper nanoparticles. *Desalination*, 388, 1-8.
- BEN-SASSON, M., ZODROW, K. R., GENGGENG, Q., KANG, Y., GIANNELIS, E. P. & ELIMELECH, M. 2014b. Surface functionalization of thin-film composite membranes with copper nanoparticles for antimicrobial surface properties. *Environ Sci Technol*, 48, 384-93.
- BERNSMANN, F., PONCHE, A., RINGWALD, C., HEMMERLÉ, J., RAYA, J., BECHINGER, B., VOEGEL, J.-C., SCHAAF, P. & BALL, V. 2009. Characterization of Dopamine–Melanin Growth on Silicon Oxide. *The Journal of Physical Chemistry C*, 113, 8234-8242.
- BJARNSHOLT, T., CIOFU, O., MOLIN, S., GIVSKOV, M. & HØIBY, N. 2013. *Applying insights from biofilm biology to drug development - can a new approach be developed?* *Nat Rev Drug Discov*.
- CADOTTE, J. E., PETERSEN, R. J., LARSON, R. E. & ERICKSON, E. E. 1980. A new thin-film composite seawater reverse osmosis membrane. *Desalination*, 32, 25-31.
- CHAN, W.-F., MARAND, E. & MARTIN, S. M. 2016. Novel zwitterion functionalized carbon

nanotube nanocomposite membranes for improved RO performance and surface anti-biofouling resistance. *Journal of Membrane Science*, 509, 125-137.

CHEN, S., LI, L., ZHAO, C. & ZHENG, J. 2010. Surface hydration: Principles and applications toward low-fouling/nonfouling biomaterials. *Polymer*, 51, 5283-5293.

CHENG, C., LI, S., ZHAO, W., WEI, Q., NIE, S., SUN, S. & ZHAO, C. 2012. The hydrodynamic permeability and surface property of polyethersulfone ultrafiltration membranes with mussel-inspired polydopamine coatings. *Journal of Membrane Science*, 417-418, 228-236.

CHOI, W., CHOI, J., BANG, J. & LEE, J.-H. 2013. Layer-by-Layer Assembly of Graphene Oxide Nanosheets on Polyamide Membranes for Durable Reverse-Osmosis Applications. *ACS Applied Materials & Interfaces*, 5, 12510-12519.

CHUDOBOVA, D., NEJDL, L., GUMULEC, J., KRYSTOFOVA, O., RODRIGO, M., KYNICKY, J., RUTTKAY-NEDECKY, B., KOPEL, P., BABULA, P., ADAM, V. & KIZEK, R. 2013. Complexes of Silver(I) Ions and Silver Phosphate Nanoparticles with Hyaluronic Acid and/or Chitosan as Promising Antimicrobial Agents for Vascular Grafts. *International Journal of Molecular Sciences*, 14, 13592.

CUI, J., YAN, Y., SUCH, G. K., LIANG, K., OCHS, C. J., POSTMA, A. & CARUSO, F. 2012. Immobilization and Intracellular Delivery of an Anticancer Drug Using Mussel-Inspired Polydopamine Capsules. *Biomacromolecules*, 13, 2225-2228.

DING, Y. H., FLOREN, M. & TAN, W. 2016. Mussel-inspired polydopamine for bio-surface functionalization. *Biosurface and Biotribology*, 2, 121-136.

DU, J., BANDARA, H. M. H. N., DU, P., HUANG, H., HOANG, K., NGUYEN, D., MOGARALA, S. V. & SMYTH, H. D. C. 2015. Improved Biofilm Antimicrobial Activity of Polyethylene Glycol Conjugated Tobramycin Compared to Tobramycin in *Pseudomonas aeruginosa* Biofilms. *Molecular Pharmaceutics*, 12, 1544-1553.

DU, X., LI, L., LI, J., YANG, C., FRENKEL, N., WELLE, A., HEISLER, S., NEFEDOV, A., GRUNZE, M. & LEVKIN, P. 2014. *UV-Triggered Dopamine Polymerization: Control of Polymerization, Surface Coating, and Photopatterning*.

ELIMELECH, M., XIAOHUA, Z., CHILDRESS, A. E. & SEUNGKWAN, H. 1997. Role of membrane surface morphology in colloidal fouling of cellulose acetate and composite aromatic polyamide reverse osmosis membranes. *Journal of Membrane Science*, 127, 101-109.

FREGER, V., GILRON, J. & BELFER, S. 2002. TFC polyamide membranes modified by grafting of hydrophilic polymers: an FT-IR/AFM/TEM study. *Journal of Membrane Science*, 209, 283-292.

H. LIN, N., KIM, M., T. LEWIS, G. & COHEN, Y. 2010. *Polymer surface nano-structuring of reverse osmosis membranes for fouling resistance and improved flux performance*.

HADDAD, J., KOTRA, L. P., LLANO-SOTELO, B., KIM, C., AZUCENA, E. F., LIU, M., VAKULENKO, S. B., CHOW, C. S. & MOBASHERY, S. 2002. Design of Novel Antibiotics that Bind to the Ribosomal Acyltransfer Site. *Journal of the American Chemical Society*, 124, 3229-3237.

HAN, J.-L., XIA, X., TAO, Y., YUN, H., HOU, Y.-N., ZHAO, C.-W., LUO, Q., CHENG, H.-Y. & WANG, A.-J. 2016. Shielding membrane surface carboxyl groups by covalent-binding graphene oxide to improve anti-fouling property and the simultaneous promotion of flux. *Water Research*, 102, 619-628.

- HE, L., DUMÉE, L. F., FENG, C., VELLEMAN, L., REIS, R., SHE, F., GAO, W. & KONG, L. 2015. Promoted water transport across graphene oxide–poly(amide) thin film composite membranes and their antibacterial activity. *Desalination*, 365, 126-135.
- HE, M., GAO, K., ZHOU, L., JIAO, Z., WU, M., CAO, J., YOU, X., CAI, Z., SU, Y. & JIANG, Z. 2016. Zwitterionic materials for antifouling membrane surface construction. *Acta Biomaterialia*, 40, 142-152.
- HEGAB, H. M., ELMEKAWY, A., BARCLAY, T. G., MICHELMORE, A., ZOU, L., SAINT, C. P. & GINIC-MARKOVIC, M. 2016. *Effective in-situ chemical surface modification of forward osmosis membranes with polydopamine-induced graphene oxide for biofouling mitigation*. 385.
- HU, Y., LU, K., YAN, F., SHI, Y., YU, P., YU, S., LI, S. & GAO, C. 2016. Enhancing the performance of aromatic polyamide reverse osmosis membrane by surface modification via covalent attachment of polyvinyl alcohol (PVA). *Journal of Membrane Science*, 501, 209-219.
- J. MILLER, D., R. DREYER, D., W. BIELAWSKI, C., R. PAUL, D. & D. FREEMAN, B. 2016. *Surface Modification of Water Purification Membranes: a Review*.
- JIANG, J., ZHU, L., ZHU, L., ZHU, B. & XU, Y. 2011. Surface Characteristics of a Self-Polymerized Dopamine Coating Deposited on Hydrophobic Polymer Films. *Langmuir*, 27, 14180-14187.
- JIANG, S., LI, Y. & LADEWIG, B. P. 2017. A review of reverse osmosis membrane fouling and control strategies. *Science of The Total Environment*, 595, 567-583.
- JOOST, U., JUGANSON, K., VISNAPUU, M., MORTIMER, M., KAHRU, A., NÕMMISTE, E., JOOST, U., KISAND, V. & IVASK, A. 2015. Photocatalytic antibacterial activity of nano-TiO<sub>2</sub> (anatase)-based thin films: Effects on Escherichia coli cells and fatty acids. *Journal of Photochemistry and Photobiology B: Biology*, 142, 178-185.
- KANG, G.-D. & CAO, Y.-M. 2012. Development of antifouling reverse osmosis membranes for water treatment: A review. *Water Research*, 46, 584-600.
- KANG, G., YU, H., LIU, Z. & CAO, Y. 2011. Surface modification of a commercial thin film composite polyamide reverse osmosis membrane by carbodiimide-induced grafting with poly(ethylene glycol) derivatives. *Desalination*, 275, 252-259.
- KARKHANECHI, H., RAZI, F., SAWADA, I., TAKAGI, R., OHMUKAI, Y. & MATSUYAMA, H. 2013. Improvement of antibiofouling performance of a reverse osmosis membrane through biocide release and adhesion resistance. *Separation and Purification Technology*, 105, 106-113.
- KARKHANECHI, H., TAKAGI, R. & MATSUYAMA, H. 2014a. Biofouling resistance of reverse osmosis membrane modified with polydopamine. *Desalination*, 336, 87-96.
- KARKHANECHI, H., TAKAGI, R. & MATSUYAMA, H. 2014b. Enhanced antibiofouling of RO membranes via polydopamine coating and polyzwitterion immobilization. *Desalination*, 337, 23-30.
- KASEMSET, S., LEE, A., MILLER, D. J., FREEMAN, B. D. & SHARMA, M. M. 2013. Effect of polydopamine deposition conditions on fouling resistance, physical properties, and permeation properties of reverse osmosis membranes in oil/water separation. *Journal of Membrane Science*, 425-426, 208-216.
- KHARAGHANI, D., KEE JO, Y., KHAN, M. Q., JEONG, Y., CHA, H. J. & KIM, I. S. 2018. Electrospun antibacterial polyacrylonitrile nanofiber membranes functionalized with silver nanoparticles by a facile wetting method. *European Polymer Journal*, 108, 69-75.

- KIM, S. H., KWAK, S.-Y., SOHN, B.-H. & PARK, T. H. 2003. Design of TiO<sub>2</sub> nanoparticle self-assembled aromatic polyamide thin-film-composite (TFC) membrane as an approach to solve biofouling problem. *Journal of Membrane Science*, 211, 157-165.
- LEE, H., DELLATORE, S. M., MILLER, W. M. & MESSERSMITH, P. B. 2007. Mussel-Inspired Surface Chemistry for Multifunctional Coatings. *Science*, 318, 426-30.
- LI, D. & WANG, H. 2010. Recent developments in reverse osmosis desalination membranes. *Journal of Materials Chemistry*, 20, 4551.
- LI, X., SOTTO, A., LI, J. & VAN DER BRUGGEN, B. 2017. Progress and perspectives for synthesis of sustainable antifouling composite membranes containing in situ generated nanoparticles. *Journal of Membrane Science*, 524, 502-528.
- LIAO, Y., WANG, Y., FENG, X., WANG, W., XU, F. & ZHANG, L. 2010. Antibacterial surfaces through dopamine functionalization and silver nanoparticle immobilization. *Materials Chemistry and Physics*, 121, 534-540.
- LIU, S., ZENG, T. H., HOFMANN, M., BURCOMBE, E., WEI, J., JIANG, R., KONG, J. & CHEN, Y. 2011. Antibacterial Activity of Graphite, Graphite Oxide, Graphene Oxide, and Reduced Graphene Oxide: Membrane and Oxidative Stress. *ACS Nano*, 5, 6971-6980.
- LOEB, S. & SOURIRAJAN, S. 1963. Sea Water Demineralization by Means of an Osmotic Membrane. *Saline Water Conversion—II*. AMERICAN CHEMICAL SOCIETY.
- LOUIE, J. S., PINNAU, I. & REINHARD, M. 2011. Effects of surface coating process conditions on the water permeation and salt rejection properties of composite polyamide reverse osmosis membranes. *Journal of Membrane Science*, 367, 249-255.
- MA, W., SOROUSH, A., LUONG, T. V. A. & RAHAMAN, M. S. 2017. Cysteamine- and graphene oxide-mediated copper nanoparticle decoration on reverse osmosis membrane for enhanced anti-microbial performance. *Journal of Colloid and Interface Science*, 501, 330-340.
- MA, W., SOROUSH, A., VAN ANH LUONG, T., BRENNAN, G., RAHAMAN, M. S., ASADISHAD, B. & TUFENKJI, N. 2016. Spray- and spin-assisted layer-by-layer assembly of copper nanoparticles on thin-film composite reverse osmosis membrane for biofouling mitigation. *Water Res*, 99, 188-199.
- MARRÉ TIRADO, M. L., BASS, M., PIATKOVSKY, M., ULBRICHT, M., HERZBERG, M. & FREGIER, V. 2016. Assessing biofouling resistance of a polyamide reverse osmosis membrane surface-modified with a zwitterionic polymer. *Journal of Membrane Science*, 520, 490-498.
- MCCLOSKEY, B. D., PARK, H. B., JU, H., ROWE, B. W., MILLER, D. J., CHUN, B. J., KIN, K. & FREEMAN, B. D. 2010. Influence of polydopamine deposition conditions on pure water flux and foulant adhesion resistance of reverse osmosis, ultrafiltration, and microfiltration membranes. *Polymer*, 51, 3472-3485.
- MCCLOSKEY, B. D., PARK, H. B., JU, H., ROWE, B. W., MILLER, D. J. & FREEMAN, B. D. 2012. A bioinspired fouling-resistant surface modification for water purification membranes. *Journal of Membrane Science*, 413-414, 82-90.
- MENG, J., CAO, Z., NI, L., ZHANG, Y., WANG, X., ZHANG, X. & LIU, E. 2014. A novel salt-responsive TFC RO membrane having superior antifouling and easy-cleaning properties. *Journal of Membrane Science*, 461, 123-129.

- MILLER, D. J., HUANG, X., LI, H., KASEMSET, S., LEE, A., AGNIHOTRI, D., HAYES, T., PAUL, D. R. & FREEMAN, B. D. 2013. Fouling-resistant membranes for the treatment of flowback water from hydraulic shale fracturing: A pilot study. *Journal of Membrane Science*, 437, 265-275.
- MISDAN, N., ISMAIL, A. F. & HILAL, N. 2016. Recent advances in the development of (bio)fouling resistant thin film composite membranes for desalination. *Desalination*, 380, 105-111.
- MÜLLER, M. & KEBLER, B. 2011. Deposition from Dopamine Solutions at Ge Substrates: An in Situ ATR-FTIR Study. *Langmuir*, 27, 12499-12505.
- NIKKOLA, J., LIU, X., LI, Y., RAULIO, M., ALAKOMI, H.-L., WEI, J. & TANG, C. Y. 2013. Surface modification of thin film composite RO membrane for enhanced anti-biofouling performance. *Journal of Membrane Science*, 444, 192-200.
- ONG, C. S., GOH, P. S., LAU, W. J., MISDAN, N. & ISMAIL, A. F. 2016. Nanomaterials for biofouling and scaling mitigation of thin film composite membrane: A review. *Desalination*, 393, 2-15.
- PAN, Y., MA, L., LIN, S., ZHANG, Y., CHENG, B. & MENG, J. 2016. One-step bimodel grafting via a multicomponent reaction toward antifouling and antibacterial TFC RO membranes. *Journal of Materials Chemistry A*, 4, 15945-15960.
- PARK, H. M., JEE, K. Y. & LEE, Y. T. 2017. Preparation and characterization of a thin-film composite reverse osmosis membrane using a polysulfone membrane including metal-organic frameworks. *Journal of Membrane Science*, 541, 510-518.
- PENG, H.-P., LIANG, R.-P., ZHANG, L. & QIU, J.-D. 2013. Facile preparation of novel core-shell enzyme-Au-polydopamine-Fe<sub>3</sub>O<sub>4</sub> magnetic bionanoparticles for glucosesensor. *Biosensors and Bioelectronics*, 42, 293-299.
- PIERCHALA, M. K., MAKAREMI, M., TAN, H. L., PUSHPAMALAR, J., MUNIYANDY, S., SOLOUK, A., LEE, S. M. & PASBAKSH, P. 2018. Nanotubes in nanofibers: Antibacterial multilayered polylactic acid/halloysite/gentamicin membranes for bone regeneration application. *Applied Clay Science*, 160, 95-105.
- QIU, W.-Z., YANG, H.-C. & XU, Z.-K. 2018. Dopamine-assisted co-deposition: An emerging and promising strategy for surface modification. *Advances in Colloid and Interface Science*, 256, 111-125.
- R CHOUDHURY, R., GOHIL, J., MOHANTY, S. & K. NAYAK, S. 2017. *Antifouling, Fouling Release and Antimicrobial Materials for Surface Modification of Reverse Osmosis and Nanofiltration Membranes*.
- SAFARPOUR, M., KHATAEE, A. & VATANPOUR, V. 2015. Thin film nanocomposite reverse osmosis membrane modified by reduced graphene oxide/TiO<sub>2</sub> with improved desalination performance. *Journal of Membrane Science*, 489, 43-54.
- SAGLE, A. C., VAN WAGNER, E. M., JU, H., MCCLOSKEY, B. D., FREEMAN, B. D. & SHARMA, M. M. 2009. PEG-coated reverse osmosis membranes: Desalination properties and fouling resistance. *Journal of Membrane Science*, 340, 92-108.
- SHAO, F., XU, C., JI, W., DONG, H., SUN, Q., YU, L. & DONG, L. 2017. Layer-by-layer self-assembly TiO<sub>2</sub> and graphene oxide on polyamide reverse osmosis membranes with improved membrane durability. *Desalination*, 423, 21-29.

- SHIRAZI, S., LIN, C.-J. & CHEN, D. 2010. Inorganic fouling of pressure-driven membrane processes — A critical review. *Desalination*, 250, 236-248.
- SILEIKA, T. S., KIM, H.-D., MANIAK, P. & MESSERSMITH, P. B. 2011. Antibacterial Performance of Polydopamine-Modified Polymer Surfaces Containing Passive and Active Components. *ACS Applied Materials & Interfaces*, 3, 4602-4610.
- SU, L., YU, Y., ZHAO, Y., LIANG, F. & ZHANG, X. 2016. Strong Antibacterial Polydopamine Coatings Prepared by a Shaking-assisted Method. *Scientific Reports*, 6, 24420.
- UDDIN, J., UEDA, K., SIWU, E. R. O., KITA, M. & UEMURA, D. 2006. Cytotoxic labdane alkaloids from an ascidian *Lissoclinum* sp.: Isolation, structure elucidation, and structure–activity relationship. *Bioorganic & Medicinal Chemistry*, 14, 6954-6961.
- VAN WAGNER, E. M., SAGLE, A. C., SHARMA, M. M., LA, Y.-H. & FREEMAN, B. D. 2011a. Surface modification of commercial polyamide desalination membranes using poly(ethylene glycol) diglycidyl ether to enhance membrane fouling resistance. *Journal of Membrane Science*, 367, 273-287.
- VAN WAGNER, E. M., SAGLE, A. C., SHARMA, M. M., LA, Y.-H. & FREEMAN, B. D. 2011b. Surface modification of commercial polyamide desalination membranes using poly(ethylene glycol) diglycidyl ether to enhance membrane fouling resistance. *Journal of Membrane Science*, 367, 273-287.
- VRIJENHOEK, E. M., HONG, S. & ELIMELECH, M. 2001. Influence of membrane surface properties on initial rate of colloidal fouling of reverse osmosis and nanofiltration membranes. *Journal of Membrane Science*, 188, 115-128.
- WANG, J., WANG, Z. & WANG, S. 2015. *Improving the water flux and bio-fouling resistance of reverse osmosis (RO) membrane through surface modification by zwitterionic polymer*.
- WANG, Y., WANG, Z., HAN, X., WANG, J. & WANG, S. 2017. Improved flux and anti-biofouling performances of reverse osmosis membrane via surface layer-by-layer assembly. *Journal of Membrane Science*, 539, 403-411.
- WANG, Y., WANG, Z., WANG, J. & WANG, S. 2018. Triple antifouling strategies for reverse osmosis membrane biofouling control. *Journal of Membrane Science*, 549, 495-506.
- WEI, Q., ZHANG, F., LI, J., LI, B. & ZHAO, C. 2010a. Oxidant-induced dopamine polymerization for multifunctional coatings. *Polymer Chemistry*, 1, 1430-1433.
- WEI, X., WANG, Z., CHEN, J., WANG, J. & WANG, S. 2010b. A novel method of surface modification on thin-film-composite reverse osmosis membrane by grafting hydantoin derivative. *Journal of Membrane Science*, 346, 152-162.
- XU, J., WANG, Z., WANG, J. & WANG, S. 2015. Positively charged aromatic polyamide reverse osmosis membrane with high anti-fouling property prepared by polyethylenimine grafting. *Desalination*, 365, 398-406.
- YANG, H.-C., LIAO, K.-J., HUANG, H., WU, Q.-Y., WAN, L.-S. & XU, Z.-K. 2014. Mussel-inspired modification of a polymer membrane for ultra-high water permeability and oil-in-water emulsion separation. *Journal of Materials Chemistry A*, 2, 10225-10230.
- YANG, H.-C., WALDMAN, R., WU, M., HOU, J., CHEN, L., B. DARLING, S. & XU, Z.-K. 2018. *Membranes: Dopamine: Just the Right Medicine for Membranes (Adv. Funct. Mater. 8/2018)*.

- YANG, H.-C., WU, M., LI, Y.-J., CHEN, Y., WAN, L.-S. & XU, Z.-K. 2016. *Effects of polyethyleneimine molecular weight and proportion on the membrane hydrophilization by codepositing with dopamine*.
- YIN, J., YANG, Y., HU, Z. & DENG, B. 2013. Attachment of silver nanoparticles (AgNPs) onto thin-film composite (TFC) membranes through covalent bonding to reduce membrane biofouling. *Journal of Membrane Science*, 441, 73-82.
- YIN, J., ZHU, G. & DENG, B. 2016. Graphene oxide (GO) enhanced polyamide (PA) thin-film nanocomposite (TFN) membrane for water purification. *Desalination*, 379, 93-101.
- YU, S., YAO, G., DONG, B., ZHU, H., PENG, X., LIU, J., LIU, M. & GAO, C. 2013. Improving fouling resistance of thin-film composite polyamide reverse osmosis membrane by coating natural hydrophilic polymer sericin. *Separation and Purification Technology*, 118, 285-293.
- ZAMANI, F., ULLAH, A., AKHONDI, E., TANUDJAJA, H. J., CORNELISSEN, E. R., HONCIUC, A., FANE, A. G. & CHEW, J. W. 2016. Impact of the surface energy of particulate foulants on membrane fouling. *Journal of Membrane Science*, 510, 101-111.
- ZHANG, R.-X., BRAEKEN, L., LIU, T.-Y., LUIS, P., WANG, X.-L. & VAN DER BRUGGEN, B. 2017. Remarkable Anti-Fouling Performance of TiO<sub>2</sub>-Modified TFC Membranes with Mussel-Inspired Polydopamine Binding. *Applied Sciences*, 7, 81.
- ZHANG, R.-X., BRAEKEN, L., LUIS, P., WANG, X.-L. & VAN DER BRUGGEN, B. 2013. Novel binding procedure of TiO<sub>2</sub> nanoparticles to thin film composite membranes via self-polymerized polydopamine. *Journal of Membrane Science*, 437, 179-188.
- ZHANG, R., SU, Y., ZHAO, X., LI, Y., ZHAO, J. & JIANG, Z. 2014. A novel positively charged composite nanofiltration membrane prepared by bio-inspired adhesion of polydopamine and surface grafting of poly(ethylene imine). *Journal of Membrane Science*, 470, 9-17.
- ZHAO, X., ZHANG, R., LIU, Y., HE, M., SU, Y., GAO, C. & JIANG, Z. Antifouling membrane surface construction: Chemistry plays a critical role. *Journal of Membrane Science*.
- ZHAO, X., ZHANG, R., LIU, Y., HE, M., SU, Y., GAO, C. & JIANG, Z. 2018. Antifouling membrane surface construction: Chemistry plays a critical role. *Journal of Membrane Science*, 551, 145-171.
- ZHOU, Y.-Z., CAO, Y., LIU, W., CHU, C. H. & LI, Q.-L. 2012. Polydopamine-Induced Tooth Remineralization. *ACS Applied Materials & Interfaces*, 4, 6901-6910.
- ZHU, X., BAI, R., WEE, K.-H., LIU, C. & TANG, S.-L. 2010. Membrane surfaces immobilized with ionic or reduced silver and their anti-biofouling performances. *Journal of Membrane Science*, 363, 278-286.
- ZOU, L., VIDALIS, I., STEELE, D., MICHELMORE, A., LOW, S. P. & VERBERK, J. Q. J. C. 2011. Surface hydrophilic modification of RO membranes by plasma polymerization for low organic fouling. *Journal of Membrane Science*, 369, 420-428.